

# **Nanocomposites for medical applications**

Kateryna O. Filatova, Ph.D.

Doctoral Thesis Summary



# Univerzita Tomáše Bati ve Zlíně

## Fakulta technologická

Doctoral Thesis Summary

### **Nanocomposites for medical applications**

#### **Nanokompozity pro medicínské aplikace**

Author: **Kateryna O. Filatova, Ph.D.**

Degree program: P2808 / Chemistry and Materials Technology

Degree course: 2808V006 / Technology of Macromolecular Compounds

Supervisor: prof. Ing. Vladimír Sedlařík, Ph.D.

Reviewer: RNDr. Jiří Zedník, Ph.D.

Reviewer: prof. Ing. *et* Ing. Ivo Kuřitka, Ph.D. *et* Ph.D.

Zlín, March 2024

© Kateryna O. Filatova

Published by **Tomas Bata University in Zlín** in the Edition **Doctoral Thesis Summary**.

The publication was issued in the year 2024

Key words in Czech: *nanokompozity, částice oxidu křemičitého, plnění léčiv, uvolňování léčiv, biologická dostupnost, biokompatibilita a toxicita, kontrolované/cílené dodávání léčiva.*

Key words: *nanocomposites, silica particles, drug loading, release study, bioavailability, biocompatibility and toxicity, controlled/targeted drug delivery.*

Full text of the doctoral thesis is available in the Library of TBU in Zlín.

ISBN: 978-80-7678-275-4



## **ABSTRACT**

This thesis is focused on fabrication of hybrid (organic-inorganic) nanocomposites using Silica-based particles for their application in medicine. For that purpose, a detailed overview of the current state of art in the field of nanocomposite materials, with a particular attention to the preparation, characterization, biocompatibility of Silica-based nanocomposites, and conventional issues related to that matter was performed. Besides that, the main objectives have been addressed as follows: first, fabrication of Si-based carriers modified with CS and chitosan grafted polylactic acid (CS-g-PLA) as controlled drug delivery systems (DDS) were performed. After, preparation of Si particles doped with Aluminium for as DDS for poor water-soluble drugs was accomplished and potential of Si-PLA nanofibers for sustained release of bioactive compounds was described. During the realization of this thesis, Silica-based nanostructured materials were synthesized, characterized, tested on the biocompatibility issues, loaded with a model drug, physical and chemically modified on their surface, and preliminarily studied as potential medical tools analysing their interactions with biological objects for their further medical application.

## **ABSTRAKT**

Tato práce je zaměřena na výrobu hybridních (organicko-anorganických) nanokompozitů, které jsou v podobě částic na bázi křemíku (Si) určeny pro budoucí aplikace v medicíně. Za tímto účelem byl proveden podrobný přehled současného stavu v oblasti nanokompozitních materiálů, se zvláštním důrazem na přípravu, charakterizaci, biokompatibilitu nanokompozitů na bázi Si a otázky týkající se této problematiky. Hlavní cíle byly řešeny následovně: nejprve byla provedena příprava nosičů na bázi Si modifikovaného chitosanem (CS) a chitosanem s kyselinou mléčnou (CS-g-PLA), jako systémy pro řízené dodávání léčiv. Dále za tímto účelem byly připraveny částice Si s hliníkem pro léčiva, které mají špatnou rozpustnost ve vodě. Pro trvalé uvolňování bioaktivních sloučenin byl popsán potenciál nanovláken Si-PLA. Během výzkumu byla syntetizována, charakterizována a testována biokompatibilita nanokompozitů na bázi křemíkové částic s modelovým léčivem (např. methotrexate a Doxorubicine), byla realizována úprava (fyzická a chemická) jejich povrchů. Tyto nanokompozity byly studovány pomocí analýzy jejich interakci s biologickým materiálem pro potenciální využití ve farmaceutickém průmyslu.

# TABLE OF CONTENTS

ABSTRACT .....	4
ABSTRAKT .....	5
1. INTRODUCTION .....	7
2. AIM OF THE DOCTORAL THESIS .....	9
3. EXPERIMENTAL SECTION .....	10
3.1 Preparation of Si-based carriers modified with chitosan (Si-Cs) and chitosan grafted polylactic acid (Si-Cs-g-Pla) as controlled DDS. ....	10
3.2 Synthesis and characterization of Si, Si-Cs and Si-Cs-g-PLA particles	10
3.3 Preparation of functionalized Si particles in different experimental conditions and investigation of an impact of its microstructure on the drug bioavailability.....	14
3.4 Fabrication of Si-PLA nanofibers for perspective wound treatment .....	23
4. CONCLUSIONS .....	29
5. SCIENTIFIC ACHIEVEMENTS AND PRACTICAL OUTCOMES .....	33
REFERENCES.....	34
LIST OF FIGURES.....	38
LIST OF TABLES .....	39
LIST OF ABBREVIATIONS AND SYMBOLS.....	40
CURRICULUM VITAE .....	41
LIST OF PUBLICATIONS .....	42

# 1. INTRODUCTION

Drug delivery systems (DDSs) are hybrid materials comprising a carrier and a drug, which control the biological active molecules release rate and reduce the limitations occurred at the classical administration of therapeutics, especially by minimizing the side effects and bioavailability improvement [1-3].

Bioavailability refers to the extent and rate at which the active moiety (drug or metabolite) enters systemic circulation, thereby accessing the site of action. Orally administered drugs must pass through the intestinal wall and then the portal circulation to the liver; both are common sites of first-pass metabolism [4]. Thus, many drugs may be metabolized before adequate plasma concentrations are reached. Low bioavailability is most common with oral dosage forms of poorly water-soluble and poorly permeable drugs [5,6].

A good delivery system should have high drug loading efficiency, which is related to the biological active molecules – matrix interaction, in order to reduce the amount of the carrier for administration, a good control of drug release and to be able to target a specific tissue of the body [7].

Various physical and chemical formulation approaches have been studied to enhance the solubility and bioavailability of BCS class II and IV compounds such as the modification of crystal habit, drug dispersion within carriers [10], lipid-based formulations, salt and prodrug formulations, particle size reduction (micronization/nanonization), and many others [8,9].

In this context, mesoporous silica nanoparticles were identified as safe and promising pharmaceutical excipients with significant potential for drug delivery, primarily via the formation of therapeutic agent-nanoparticles based delivery systems. Because of their unique properties: biocompatibility and non-toxic behavior, biosafety, high adsorption capacity, and possibility of tailoring the release profiles based on the interactions between the guest drug molecules and silica pore surface they allow the formation of host-guest interaction with a wide range of both hydro- and lipophilic molecules [10,11]. The high specific surface area and pore volume, the ordered pore array with narrow size distribution, and the possibility to modify their architecture in order to control the biological active molecules adsorption and release kinetics. To obtain a desired matrix, the interaction between the drug and carrier must be tailored. This can be done by modifying the structural and textural properties of the mesoporous supports by using various synthesis conditions, especially different template agents, or through the modification of pores surface with organic moieties via functionalization procedures [12,13].

There are various approaches to apply SN addressing the challenge of enhancing their solubility and bioavailability. The most common methods of modifying the MSN properties include functionalization with organic groups, doping the silica framework with different atoms, or changing the morphologic and textural MSN properties [14].



Drug encapsulation: SN provide a large surface area and porous structure that allows for high drug loading. The low soluble drug can be encapsulated within the nanoparticle matrix, either by physical adsorption or by incorporating the drug within the nanoparticle during the synthesis process. This encapsulation helps to protect the drug from degradation and increases its solubility [15].

Surface modification: the surface of SN can be modified with hydrophilic functional groups or polymers to improve the solubility of the low soluble drug. These modifications increase the dispersibility of the nanoparticles and enhance their interaction with water, facilitating drug release and dissolution [16,17].

Amorphous state Formation: SN can be employed to convert crystalline low soluble drugs into their amorphous form. Amorphous drugs have higher solubility than their crystalline counterparts due to the absence of well-defined crystal structures. SN act as stabilizers, preventing drug recrystallization and maintaining the drug in its amorphous state, thereby improving its solubility and dissolution rate [10,16, 18, 19].

Controlled Release: SNs can be designed to achieve controlled release of low soluble drugs, providing sustained and prolonged drug release. The porous structure of the nanoparticles allows for the gradual diffusion of the drug, overcoming its low solubility and maintaining therapeutic concentrations over an extended period. [20].

Combination with co-solvents or surfactants: SN can be used in combination with co-solvents or surfactants to enhance the solubility of low soluble drugs. Co-solvents like ethanol or propylene glycol can be loaded within the nanoparticle pores along with the drug to improve its solubility upon release. Surfactants can also be adsorbed onto the nanoparticle surface, aiding in the formation of drug-stabilizing micelles and increasing drug solubility [21].

SN offer a versatile platform for enhancing the solubility and delivery of low soluble drugs. However, it is crucial to conduct comprehensive studies to determine the optimal formulation, drug loading, release kinetics, and long-term stability to ensure effective and safe drug delivery [22].

The most commonly used route for synthesizing silica nanoparticles is sol-gel method due to its ability to produce monodispersed with narrow-size distribution nanoparticles at mild conditions. However, a challenge in the preparation of nanocomposites is the compatibility in the mixing between the filler and organic components that could be improved through surface modification of silica with polymers, namely chitosan and PLA, along with variable processing methods for nanocomposite preparation [23].

Current work is an endeavour to investigate the capability of Si-based nanocomposites to act as a typical nanoscale material with adjustable physiochemical and biological properties, to facilitate interfacial processes involved in the delivery of various active pharmaceutical ingredients via different administration routes, thereby enhancing bioavailability [24, 25].

## **2. AIM OF THE DOCTORAL THESIS**

The current thesis are done by emphasizing tasks on the synthesis of silica nanoparticles, characterization on size- and surface-dependent properties mostly by sol-gel technique and their impact on the loading and release of bioactive compounds. Influence of microstructure on the drug release from silica particles was in the focus of attention in the thesis.

The most commonly used route for synthesizing silica nanoparticles is sol-gel method due to its ability to produce monodispersed with narrow-size distribution nanoparticles at mild conditions. However, a challenge in the preparation of nanocomposites is the compatibility in the mixing between the filler and organic components that could be improved through surface modification of silica by different routes along with variable processing methods for nanocomposite preparation.

This doctoral thesis is an endeavour to investigate the capability of Si-based nanocomposites to act as a typical nanoscale material with widely adjustable physiochemical and biological properties, either commercially available or custom-made to facilitate interfacial processes involved in the delivery of various active pharmaceutical ingredients via different administration routes, thereby enhancing bioavailability.

To accomplish these tasks, the following objectives were established:

- Preparation of Si particles in different experimental conditions.
- Investigation of an impact of microstructure on the drug release from Si particles.
- Preparation of Si-based carriers modified with chitosan and chitosan grafted polylactic acid (CS-g-PLA) as controlled DDS.
- Preparation of Si particles doped with Aluminium for as DDS for poor water-soluble drugs.
- Fabrication of Si-PLA nanofibers for potential medical application.

### **3. EXPERIMENTAL SECTION**

#### **3.1 Preparation of Si-based carriers modified with chitosan (Si-Cs) and chitosan grafted polylactic acid (Si-Cs-g-Pla) as controlled DDS.**

Nanoparticles such as SNs has been considered a promising material in the engineering of targeted drug delivery carriers due to delivering drugs in a controlled manner as a result of their large surface area, quantity of pores, adjustable diameter of such pores, and modifiable surface. However, unmodified silica particles have exhibited potential toxicity, initial large burst of drug release. To overcome such limitations, hybrid carriers based on mesoporous silica and polymers could be used as stimuli-responsive, controlled-release systems [26, 27].

Thus, synthesis of carriers comprising silica (Si) coated with pristine chitosan (Si-Cs) and chitosan grafted with polylactic acid (Si-Cs-g-PLA) and investigation of their possibility to load and release a model drug (Doxorubicin (Dox)) has been performed with this potential in mind that protective effect of the Cs-PLA copolymer coated to Si surface would effectively negate any premature release of the anticancer drugs prior to reaching the targeted site (mostly in intestine) [28, 29].

The novelty herein is that the authors report for the first time the synthesis and application of silica coated with chitosan that is crosslinked with polylactic acid (Si-Cs-g-PLA) as an effective drug carrier, and discuss the feasibility of taking advantage of the dispersion effect of porous silica, the swelling of chitosan, and the hydrophobicity, erosion and degradation of polylactic acid to postpone the drug release rate.

The aim of this work was to study the effects the surface specificity of the adsorbents and the medium pH had on the kinetic parameters of Dox adsorption, and to identify the mechanisms of the process. To reveal effect pH had on the kinetic parameters of drug adsorption, our studies were carried out at pH 4.5, 7.0, and 8.0.

#### **3.2 Synthesis and characterization of Si, Si-Cs and Si-Cs-g-PLA particles**

Si particles for drug encapsulation and further development of the drug carriers were synthesized using a sol-gel method based on a cationic CTAB-template and NH<sub>4</sub>OH catalyst in alkaline pH, under highly dilute and low surfactant conditions [19, 40, 72, and 85]. Sol-gel synthesis of mesoporous Si required a template agent due to the necessity for direct polymerization of silicates from a precursor (e.g., an ester of orthosilicic acid). To this end, tetra-alkyl oxide of silane could be applied as a source of silica. Formation of liquid-crystalline meso-phases of amphiphilic surfactant molecules served as templates for in situ polymerization

of orthosilicic acid. CTAB was removed by extraction with HCl and calcination in order to create pores on the surface of the Si spheres. This method provided synthesis of Si particles with adequate surface properties in a time-efficient manner, while also permitting lesser requirements for excipients.

The most popular means for preparing Si-Cs and Si-Cs-g-PLA particles is post-synthetic grafting of modified or unmodified Si with polymers. This is the so-called “grafting to” method, permitting in situ monomer polymerization with the growth of polymer chains from immobilized initiators [32, 46]. Grafting is commonly carried out by silylation on free ( $\equiv\text{Si-OH}$ ) and geminal silanol ( $=\text{Si}(\text{OH})_2$ ) groups. If high surface coverage with functional groups is desired, it is important to maintain a large amount of surface silanol groups after removing the surfactant.

Herein, the polymeric coating of the Si particles was performed through post-synthesis grafting of pristine Si particles with polymers, the intention being to cause different types of interaction (Figure 1), i.e. electrostatic, covalent interaction and H-bonding. The Cs-g-PLA co-polymer was prepared via modified EDC/NHS chemistry, through conjugation of low-molecular-weight PLA to Cs in order to obtain the Cs-g-PLA co-polymer.

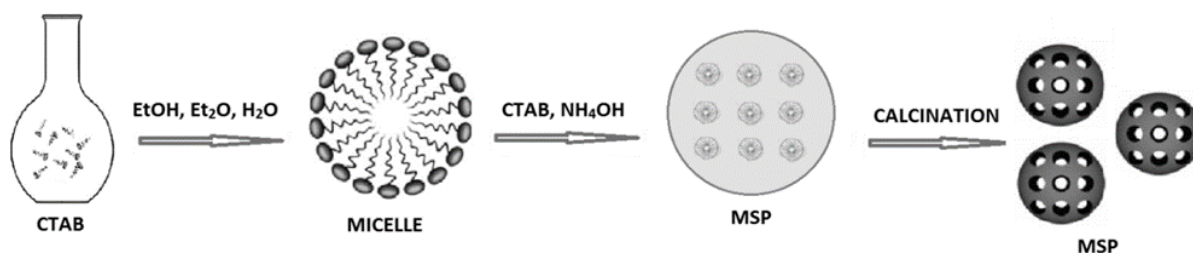


Figure 1 Schematic representation of Si particles formation.

Morphology of the particles was explored by FE-SEM and TEM analysis (Figure 2,3), which established the existence of particles with regular shape, size and surface morphology. The Si-based particles (Figure 3) exhibited a non-aggregated spherical (Si) and misshapen (Si-Cs, Si-Cs-g-PLA) morphology at an average size of 180, 200, 480 and 270 nm, respectively.

The internal structure of the carriers was investigated by TEM (Figure 3), which revealed a highly organized mesh of regular arrays of mesoporous channels and pores; these were derived as a consequence of CTAB removal during Si core synthesis. The Si-Cs carriers possessed a rough, spherical morphology of increased size, due to the polymer coating applied, while the Si-Cs-g-PLA carriers exhibited particles which were rough, irregular in shape and of enlarged size. The core shell of the polymer is visible in Figure 18, in C, D, E and F, as a compacted outer layer of different width arising though the varied amount of organic compounds grafted to the Si surface. A mesostructure is apparent, slit-like in shape and homogeneously distributed on the surface of the spheres, especially the pristine Si carrier.

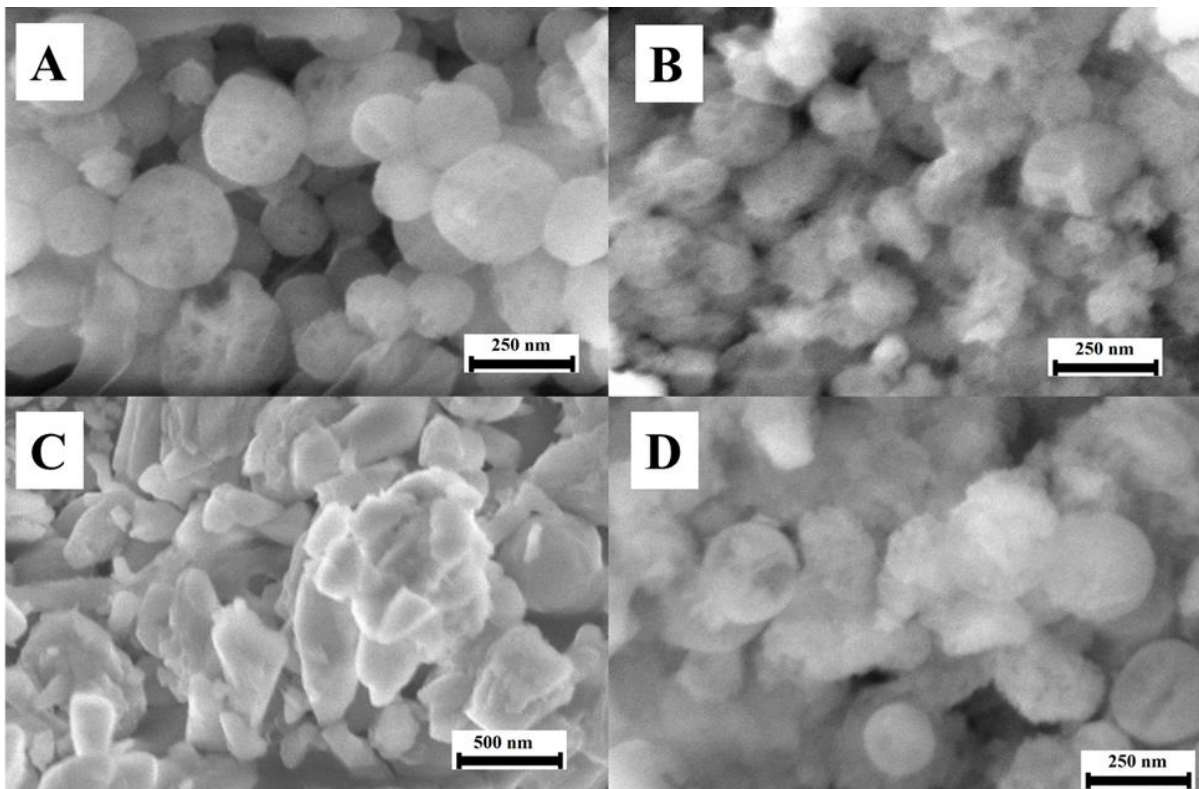


Figure 2 SEM-images of silica-based nanoparticles (Silica (A), APTES-modified Si (B), Si-Cs (C) and Si-Cs-g-PLA (D)).

Different types of elemental analysis, both involving TGA, were used to prove that a polymeric coating existed on the silica surface. Additionally, elemental analysis proved that the core shell coating on the carriers was present. DLS measurements were applied to verify physical interaction took place, due to variation in surface charge, while FTIR-ATR spectroscopy was conducted to check for chemical linkage.

DOX was chosen as the model drug due to its gastro toxicity and hydrophilicity with the aim to investigate protective properties of the carriers. It was loaded into the carriers by adsorption, after optimum conditions for dosing the drug into each carrier had been established. Moreover, the ideal time frames, pH levels and concentration conditions were discerned for loading the drug. An acidic medium was found to be the most favorable option for drug entrapment within the polymeric coated carriers and subsequent release of their contents, while a neutral or acidic medium was more suitable for release from a pristine Si carrier. Under the same conditions (pH 4.5), the Si-Cs carrier shared the exact same adsorption capacity as the Si-Cs-g-PLA carrier, despite the fact that the amount of polymer coated on the two surfaces differed. These findings to a certain extent contradicted previously published results, the latter stating that immobilized Cs exhibits a higher adsorption capacity than PLA-crosslinked Cs, this being due to the greater number of accessible adsorption sites on the Si-Cs composite and its large surface area.



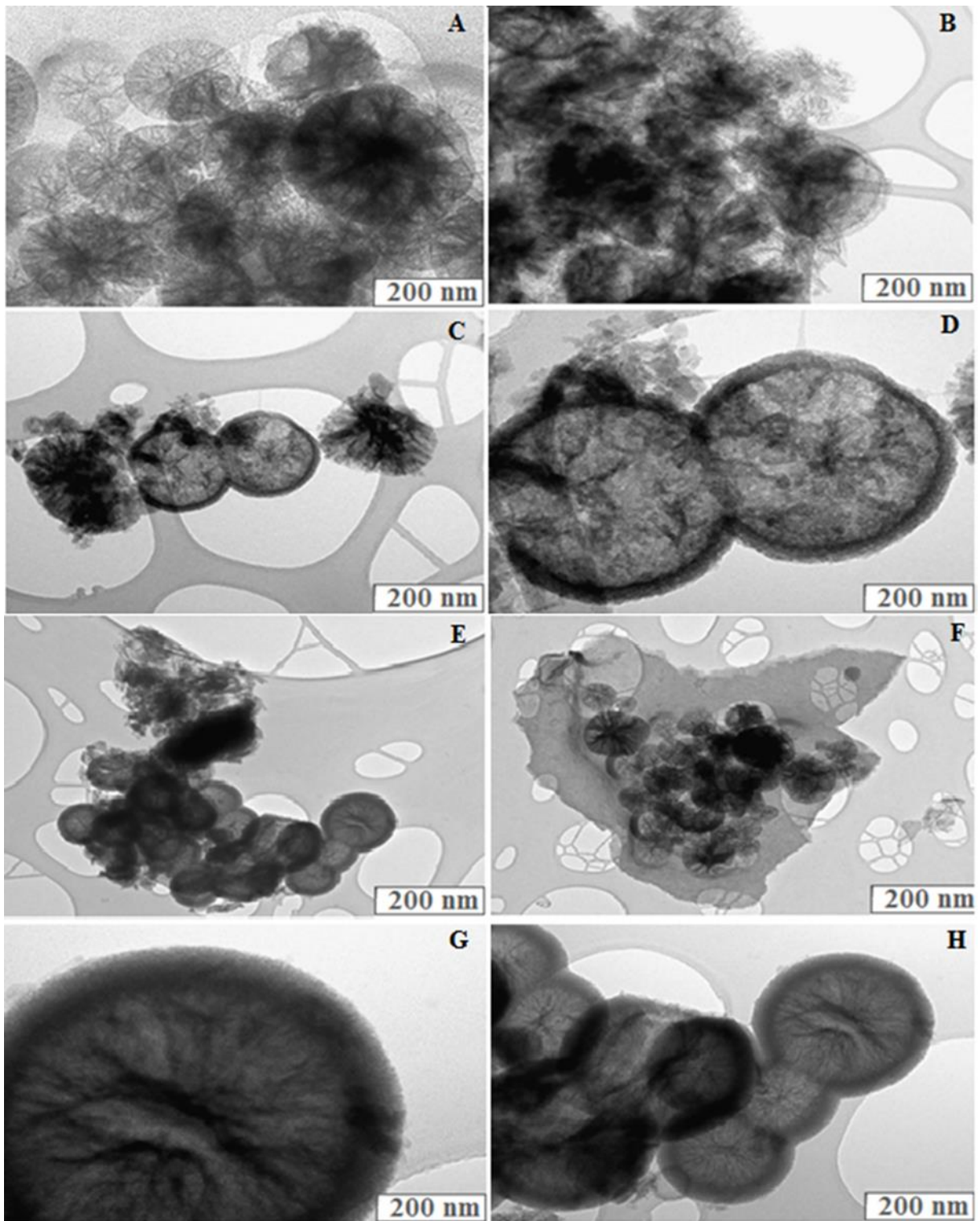


Figure 3 TEM images of silica-based particles Silica (A), Si+Dox (B), Si-Cs-g-PLA (C, D), Si- Cs (E, F, G, H).

The Si carrier demonstrated rapid and full release, achieving a high level of delivery. Its encapsulation at a different pH level and favorable release rate were characterized by the absence of an initial burst in the Si-Cs carrier, which eventually occurred after 5 h, thereby indicating that Cs played an important role in delaying the release of the drug; the absence of an initial burst effect also

proved that DOX was located inside the system and was well protected from the external medium.

Delayed release from the Si-Cs-g-PLA carrier was dependent on pH; furthermore, the ratio of DOX encapsulated and released was the same, which makes the carrier suitable for administering drugs and achieving the desired postponed effect.

The results show that the surface functionalization of Si can serve as a simple tool for controlling the loading and release of water-soluble, weak electrolyte drugs like DOX. These data mean that Si, Si-Cs, and Si-Cs-g-PLA carriers are perspective candidates for fast (Si), sustained (Si-Cs), and delayed administration of DOX.

### **3.3 Preparation of functionalized Si particles in different experimental conditions and investigation of an impact of its microstructure on the drug bioavailability.**

In this study, Al-doped mesoporous supports were synthesized by the slight modification of existing procedures [24,28], in the presence of CTAB, TTAB and DTAB as structure-directing agent. Typically, 700 mg of CTAB were dissolved in 120 mL of deionized water followed by the addition of 3.5 ml 2M aqueous NaOH solution at 120°C. Then, 35 mL of TEOS were slowly dropped for 0.5 h, under magnetic stirring in the solution containing the template agent (CTAB\_MSN). In the case of the Al\_CTAB\_MSN, a mixture of TEOS and the desired amount of  $\text{Al}[\text{OCH}(\text{CH}_3)_2]_3$  was used. A molar ratio TEOS:Al:CTAB:NaOH:H<sub>2</sub>O of 0.166:0.003:0.002:0.35:6.67 was used. The reaction mixture was stirred for 2 h to perform the precursor hydrolysis. After the white gel was hydrothermal treated for 24 h at 120°C (5 atm of Ar added). Then, the solid was filtered off, intensely washed with ethanol, deionized water, and dried at room temperature for 24 h. All the synthesized mesoporous samples were annealed at 550°C for 5 h, in air to remove the organic compounds, using a heating rate of 2°C/min. In order to evaluate the influence of various structural and textural features of the mesoporous carriers towards the adsorption and dissolution of Meth, besides the three synthesized supports, other three Al-free supports were also employed.

A fraction of the Al\_MSNS was treated in order to extract the surfactant template by Soxhlet extraction with ethanol/HCl for 24 hours. RhB and Bodipy molecules were attached covalently on the extracted samples doped with Al.

Meth was loaded on different nanoparticles supports, both silica and aluminosilicate with different Al content. We studied the influence of the textural features and the acidic nature of the mesostructured supports towards the Meth adsorption, in vitro delivery and membrane permeability.

Al-MSN-Meth solid dispersion was prepared using adsorption from solution method. X-Ray diffraction (XRD), energy-dispersive spectroscopy (EDX),

Fourier transform infrared spectroscopy analysis (FTIR) were utilized to characterize nanoformulations. In-vitro dissolution and membrane permeability examinations were applied to investigate bioavailability of the immobilized medicine.

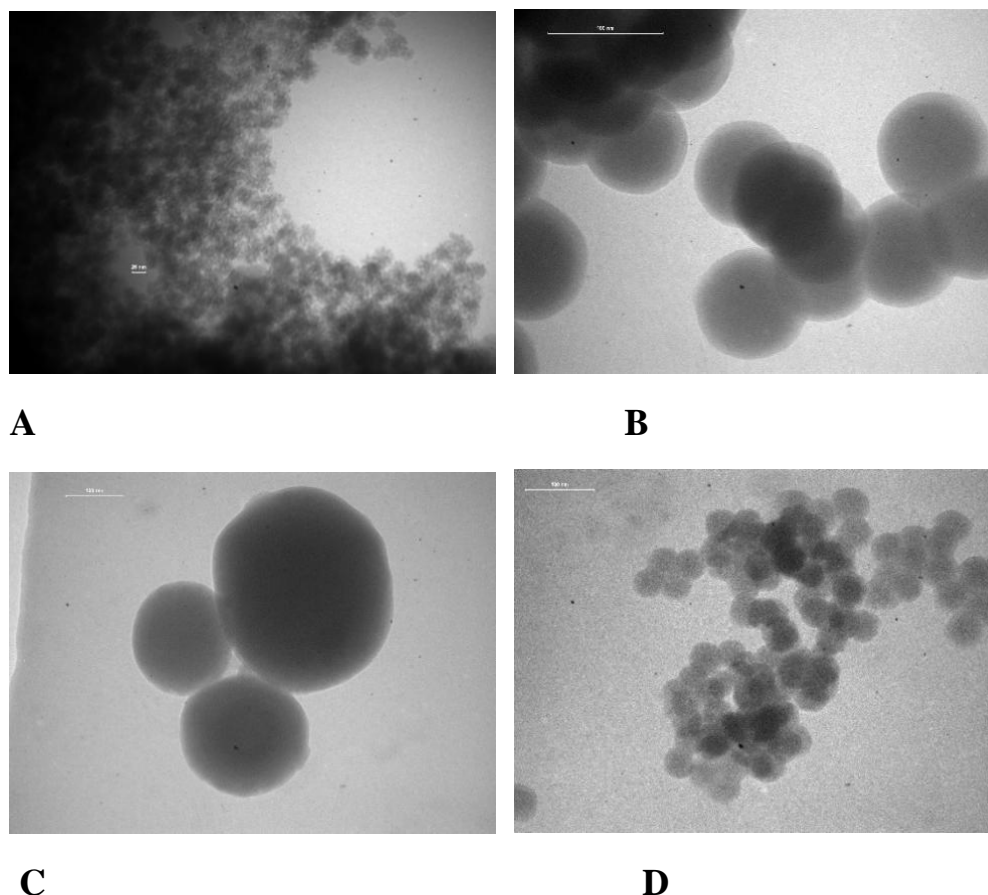


*Figure 4 Micrographs of the Al-doped MSNs: MSN-ALTAB (a, d), MSN-Al-CTAB (b), MSN-Al-DTAB (c).*

Spherical SN were synthesized by sol-gel method with further hydrothermal treatment with certain modifications of Al/Si ratio to ensure that the resulting particles are of spherical shape. After template removal, the morphology and structure of the obtained pristine spherical MSN and Al- MSNs were investigated with electron microscopy, as shown in Figure 4.

The synthesized carriers were characterized by small-angle XRD, FTIR spectra, N<sub>2</sub> adsorption/desorption isotherms, and TEM. Both the pristine carriers and drug-loaded samples were characterized in order to determine the relevant properties affecting the drug release process.

The following types of spherical Al-MSNs were obtained, as illustrated in Figure 4: unmodified (pristine) MSNs (TTAB-MSN, DTAB-MSN, and CTAB-MSN) and MSNs doped with Al (Al-MSN-TTAB, Al-MSN-DTAB, and Al-MSN-CTAB).



SEM images of Meth-loaded Al-doped MSNs confirm that they are of equal and uniform spherical shape with the size of a single particle of 45, 74 and 160 nm. Introduction of Al did not drastically distorted shape and size of particles (Table 1).

Table 1 Composition of the samples with the different Si/Al initial ratio versus acidity and a particle size.

Samples	Particles size, nm	Acidity, $\mu\text{M}$	Si/Al ratio
TTAB-MSN	45	-	-
DTAB-MSN	140	-	-
CTAB-MSN	70	-	-
Al-TTAB-MSN	45	175	85
Al-DTAB-MSN	160	596	164
Al-CTAB-MSN	74	409	143

Drug loading: As shown in Table 2, the drug loading was correlated with the structural parameters of the obtained materials and content of Al.

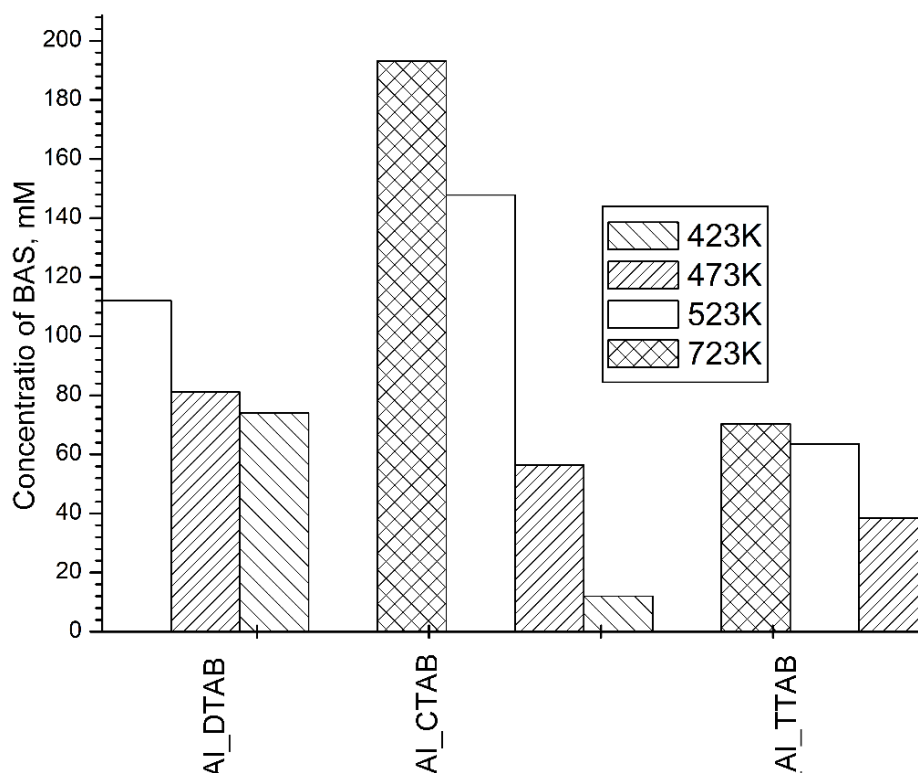


Figure 5 Acidity and morphology (size and shape) of the investigated samples (MSN\_Al\_DTAB, MSN\_Al\_CTAB and MSN\_Al\_TTAB)

*Table 2 Methotrexate storage capacities of MSNs and MSNs modified with Aluminium after interaction with Methotrexate solution*

Sample	Encapsulation efficiency at 1mg/ml	Loading capacity, mg of Meth/mg of carrier
MSNs		
MSN_TTAB	0.31	0.04
MSN_CTAB	0.47	0.10
MSN_DTAB	0.18	0.03
Al-MSNs		
Al_MSN_TTAB	0.73	0.09
Al_MSN_CTAB	0.77	0.15
Al_MSN_DTAB	0.69	0.12

Pure MSNs (MSN-CTAB, MSN-TTAB, MSN-DTAB ) showed lower adsorption capacity toward Meth than al-modified one as well as samples ( MSN-CTAB, MSN-TTAB) with with bigger pores, which are easily accessible for Meth molecules. It is worth to mention that the sorption capacities of Al-MSNs towards Meth increase with increasing pore volume (Al-MSN-CTAB with  $0.87 \text{ cm}^3\text{g}^{-1}$  and 2.52 nm pore size with loading capacity 0.15 mg/mg of carrier and Al-MSN-TTAB with  $0.56 \text{ cm}^3\text{g}^{-1}$  and 2.23 nm pore size with loading capacity 0.09 mg/mg of carrier ) and percentage content of Al (gradually decreases in the line MSN-CTAB, MSN-DTAB, and MSN-TTAB), which indicates the electrostatic interactions arising between the negatively charged pore surface and the positively charged model drug molecules as well as chemical interaction between Al and Meth with formation of supramolecular organometallic complexes takes place. The ability of Al-MSNs to take complexes with Meth follows from the amphiphilic structure of Meth due to the presence of  $-\text{COOH}$  and  $-\text{NH}_2$  groups, thus facilitating its uploading at certain pH and, potentially, release and permeability.

The current loading capacity for all carrier was established only for concentration of carrier 1mg/ml, loading volume 3 ml and amount of carrier 20 mg. Another proportions of the adsorbent and adsorbat could drive to different values. However, the purpose of a current reaserch is focused not on the quantitative assessment of the maximal loading capacity, but on the establishment differences that happens in drug loading while MSNs are doped with Al.

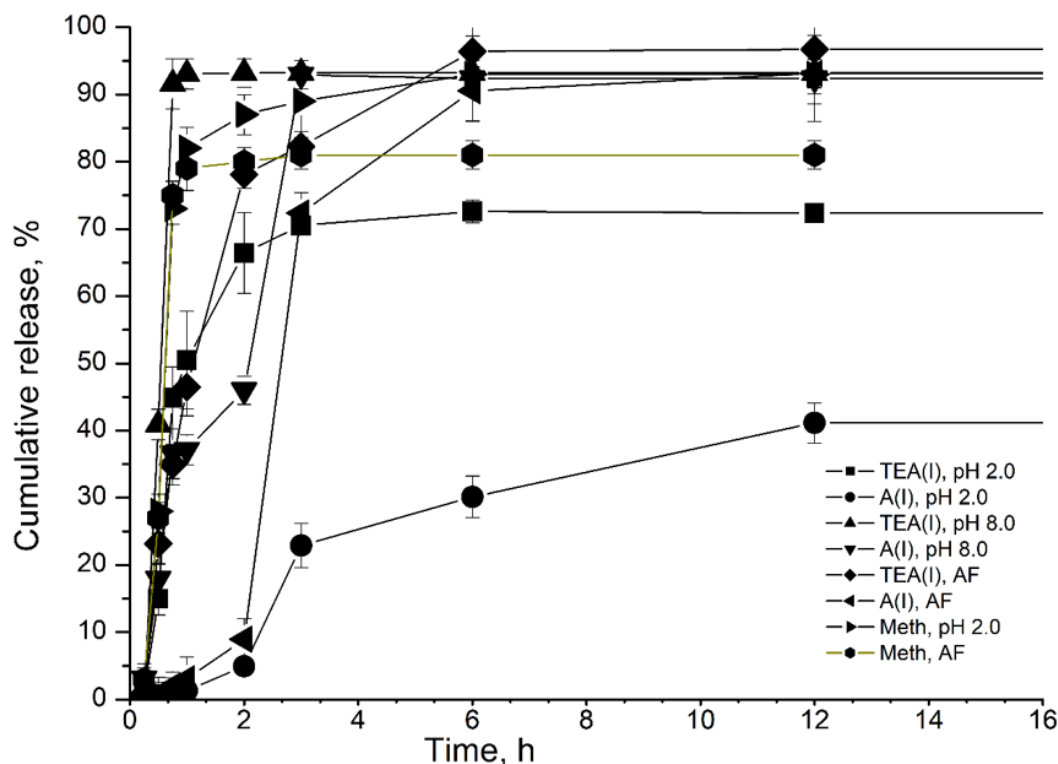


Figure 6 Dissolution profiles of Meth from Meth-loaded Al-MSN-170nm, Al-MSN-70nm and Al-MSN-35nm and crude Meth at pH 2.0 and 8.0. Each data point represents the mean  $\pm$  SD of three determinations. of Meth dissolution from Al-doped MSNs. Standard deviation was within 5% range

**In vitro dissolution:** The effect of the prepared Meth-loaded Al-MSNs formulations on the Meth dissolution rate in enzyme-free simulated intestinal (pH 8.0) and gastric (pH 2.0) fluid is shown in Figure 6. The Meth dissolution profiles were obtained at pH=2.0 and 8.0, 37°C for all samples, using the dialysis bag method and compared with the crude drug dissolution in similar conditions (Figure). The MTP dissolution through the dialysis membrane is relatively fast, reaching 90% cumulative release after 2.5 h. In contrast, the drug release kinetics from the Al-MSNs carriers is slower, signifying the fact that these mesoporous materials can control the drug delivery. However, the dissolution rate of Meth from a Meth-loaded Al-MSN carriers was significantly improved, which is of particular importance in the case of poor water-soluble drugs like Meth. The dissolution improvement may be largely attributed to the pore channels of the two carriers changing the crystalline state of Meth to an amorphous state, which is known to improve the drug solubility and dissolution rate (amorphous state of Meth after incorporation into Al-MSNs is shown on XRD). The increased dissolution rate of Meth was mostly resulted also from the reduction of drug

particle size and the improved wettability due to the interaction of drug molecules with silica surface. The formation of the less ordered drug crystals and the reduction of drug particle size were due to the spatial confinement of the pores in Al\_MSNs matrix [Effect of pore size of three-dimensionally ordered macroporous chitosan–silica matrix on solubility, drug release, and oral bioavailability of loaded-nimodipine]

It is worth noting that a faster Meth release of the drug-loaded samples was observed from the Meth-loaded Al\_MSN\_35 and Al\_MSN\_170nm carrier. The difference in release rate, which is mainly attributed to the carrier pore size, could appear weird because it was found that bigger pore size facilitates release of incorporated compounds with the pores [Effect of Aluminum Incorporation into Mesoporous Aluminosilicate Framework on Drug Release Kinetics], but not always. For instance, silica-based carriers with the largest pore size had the release rate of the drug lower than that with smaller one [Effect of pore size of three-dimensionally ordered macroporous chitosan-silica matrix on]. Such controversial results could be related to the difference in the pore volume and thus amount of loaded Meth, which was not considered as important. In our case the Meth molecules adsorbed in the narrow Al\_MSN\_35 nm sample pores in less amount comparing Al\_MSN\_170 nm have a greater chance of faster escaping from the pores and diffusing into the release medium compared with those adsorbed in the pores in bigger amount. The difference in the dissolution of Meth from Al\_MSN\_70, which is the fastest, could be contributed to the fact that pore size for this samples as well as pore volume is very low for successful loading of Meth inside the pores. Thus there is a big chance that Meth is immobilized mainly on the outer surface of the particles favouring faster release comparing with accommodated with the pores. This effect could be understood as arising from the reduced supramolecular interactions between drug molecule and the aluminosilicate pore walls, as only a fraction of Meth Al\_MSN\_70nm can be adsorbed directly within the pores.

The effect of pH on the dissolution profile of Meth from Al\_MSNs at basic pH results in dissolution fastening and increase comparing with acidic pH, which could be due to protonating of -NH<sub>2</sub> group of Meth resulting in positive charge of a molecule and further decrease of electrostatic interaction between the drug and matrix.

Certain level of dissolution (obviously less than those at basic pH) could be due to the fact that Meth is weak acid with pK. Thus, by reaching acidic pH, repulsion between acidic sites of Al-doped MSNs and Meth increases resulting in little Meth leakage.

Meth dissolution rate profile from Al-MSN-170 has two stages. During the burst stage Meth from outer surface is probably released. The dissolution at the second step is related to the drug-loaded amount inside of the pores of the carrier. The sustained release rate was found to be correlated with the steric crowding of the dissociated molecules inside the support mesopores.

**Methotrexate permeability:** Calculations of the permeability of free Meth and Meth-loaded Al-MSNs-Meth are represented in the Table 3.

*Table 3 Cumulative amount of Meth transported from A to B and B to A in MDCK-MDR cells. Experiment was performed in triplicates (n=3, p<1)*

$P_{app}(\text{Meth})(\text{BL} \rightarrow \text{AP})$	$4.40 \times 10^{-7}$
$P_{app}(\text{Meth})(\text{AP} \rightarrow \text{BL})$	$2.64 \times 10^{-4}$
$P_{app}(\text{Al-MSNs-Meth})(\text{AP} \rightarrow \text{BL})$	$9.86 \times 10^{-2}$
$P_{app}(\text{Al-MSNs-Meth})(\text{BL} \rightarrow \text{AP})$	$1.00 \times 10^{-3}$
A	373
ER	98.6

The A to B transport represented by the Papp values of Meth and Al-MSNs-Meth samples are comparable with  $2.64 \times 10^{-4}$  cm/s and  $9386 \times 10^{-2}$  cm/s, respectively. However, both samples' B to A transport (efflux) was significantly higher as well comparing with their influx rate (A to B transport), in agreement with previous assertions that Meth is subjected to P-glycoprotein (P-gp) mediated efflux, resulting in lower systemic drug concentration. In particular, the efflux ratio (B to A/A to B) of free Meth was substantially high (600). However, in addition to increased drug solubility due to the inclusion of Meth in Al-MSNs, inhibition of the P-gp driven efflux system may have contributed to increased systemic absorption, therefore enhanced permeability of Meth. Thus, SNs-based formulations effectively inhibit the P-gp efflux system of poorly water-soluble and low permeable molecules.

Herein, a promising carrier for enhanced Meth release and permeability has been designed. The effects of Al doping and MSN textural parameters on the Meth release kinetics are established. The results of in vitro studies concerning preparation, physicochemical characterization, cytotoxicity evaluation, and transport across Madin-Darby canine kidney MDR1-transfected cell line (MDCKII-MDR1) of the Al-doped mesoporous silica particles are reported.

**Nanoparticles uptake and permeability of Al-MSNs in vitro:** Therapeutic bioavailability of medicine is determined by two properties, dissolution profile (which we could characterise by in-vitro dissolution test ) and permeability through biological barriers, i.e. gemato-encephalic, gastro-intestinal, placental, dermal etc. barriers. Since Meth is mostly administered orally, we designed barrier

membrane permeability examination mostly relevant to gastro-intestinal permeability. MDCK-cells are well known to be a model biological model for gastro-intestinal and blood-brain permeability evaluation of medicines. That is why it was applied to investigate bioavailability of the immobilized Meth in cell culture laboratory. Confocal microscopy was applied to investigate possible translocation of Al-MSNs through the cell layer.

To the best of authors knowledge there were a few studies on the permeability of unmodified MSNs through MDCK-MDR cell line and no investigation on the impact of Al doping on the permeability and cell uptake of MSNs and following moderation of liberation of the drug immobilized and its interconnection with permeability of BCS IV medicines. Therefore, we evaluated the permeability of MDCK cell line for Al-MSNs and Meth permeability.

As nanoparticles in general are too large to pass through the tight cell junctions of an intact BBB and GIT (paracellular route), the expected mechanism of transport over a cell layer would rather be transcytosis (transcellular route). In order for this to take place, the particles would first have to be taken up by the cells via endocytosis, be translocated across the cell, and, ultimately, exocytosed.

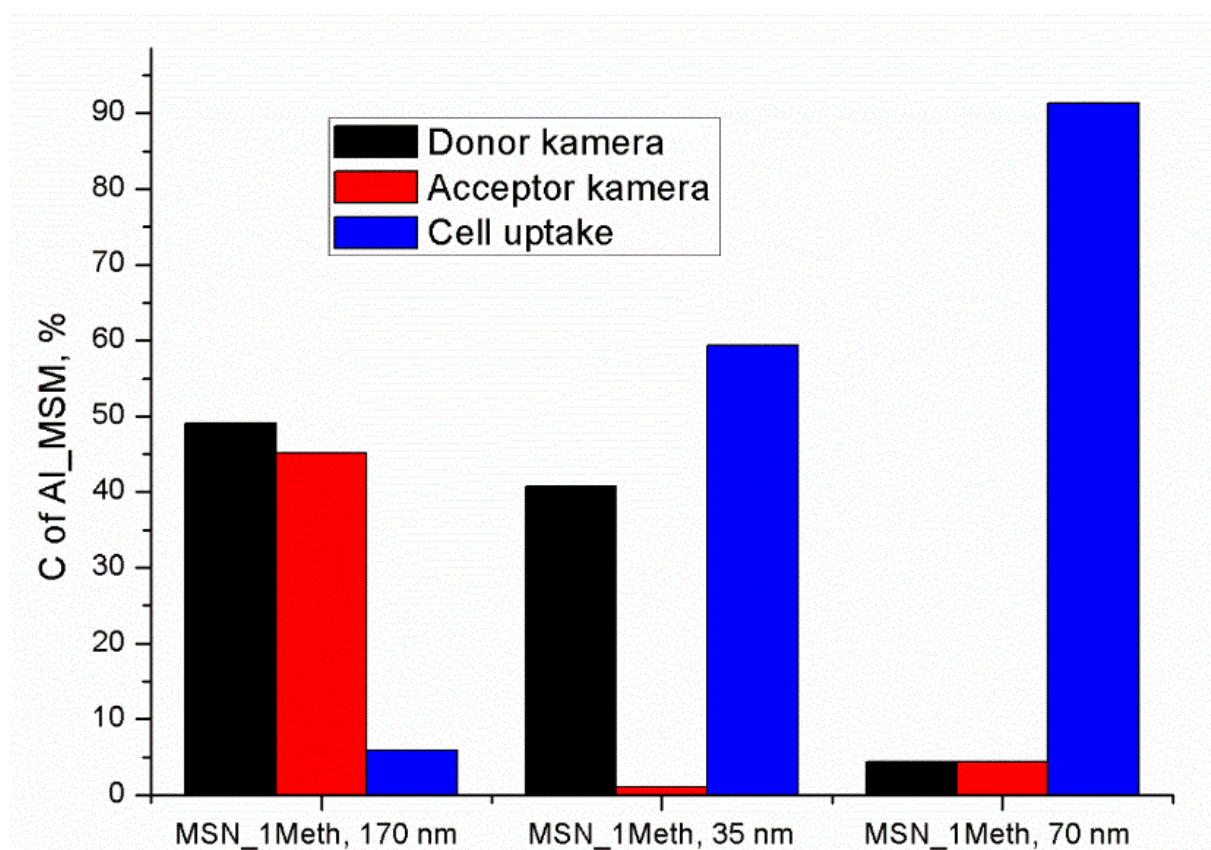
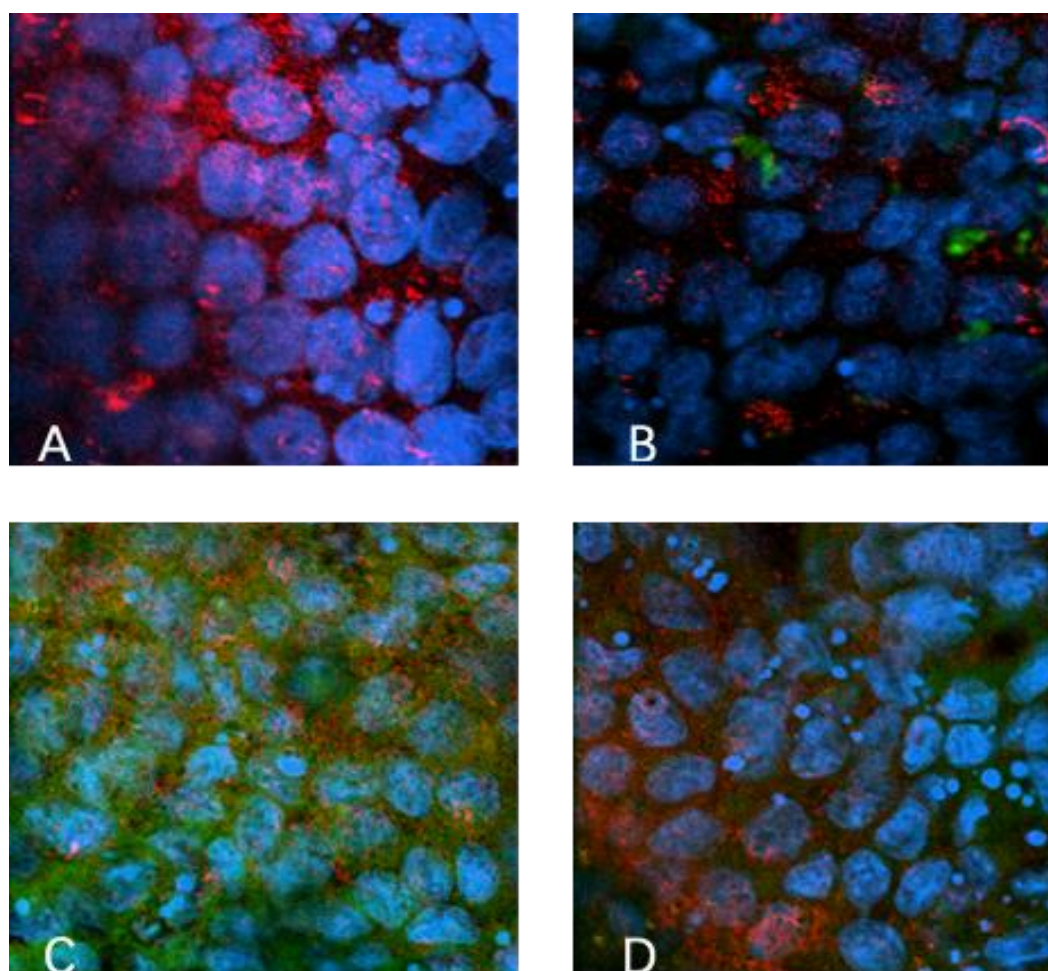


Figure 7 Transport of different Al-MSNs across MDCK MDR1 monolayers in serum-free medium. Dye-labelled Al-MSNs were applied at a concentration of 50  $\mu\text{g/ml}$ . Data represent the mean apparent permeability ( $P_{app}$ ) of MSN ( $n = 3$ ) at the time point 48 hours, corrected for the loss of Al-MSNs in the upper compartment (non-permeated Al-MSNs) and associated (cellular uptake) with the cells.



Figure 7 depicts transportation of different Al-MSNs across MDCK MDR1 monolayers in serum-free medium. MDCK-MDR1 monolayers were incubated with 50  $\mu\text{g}/\text{ml}$  MSNs in serum-free medium, with their subsequent detection in the samples of the basolateral compartment. MDCK-MDR1 cells were chosen as a suitable biological barrier permeability model in the transport study because of their barrier properties. Detection was based on fluorescence emitted by the fluorescent tag (Bodipy) used to label the Al-MSNs. Transport of different Al-MSNs across MDCK-MDR monolayer differed significantly at the studied concentration with robust uptake of the nanoparticles of 70 nm size and almost all quantity of 170 nm nanoparticles stored either in donor or acceptor camera and almost no permeation of nanoparticles of 45 nm size that were left either in donor camera or associated to the cells. Al-MSNs of 70 nm size (sample MSNs-TTAB) was chosen further for Meth release assessment because negligible amount of these nanoparticles were left in donor camera within tested time.



*Figure 8 Confocal images of MDCK-MDR1 cells incubated for 24 hours with Al-MSNs applied at a concentration of 50  $\mu\text{g}/\text{ml}$  in serum-free medium. Nuclei stained with Hoechst 33258 (blue). Al-MSNs labeled with Bodipy (green). F-actin stained with phalloidin (red) a) reference; b) MSN-CTAB (160nm) in MDCK MDR1; c) MSN-DTAB (70nm) in MDCK MDR1; d) MSN-TTAB (45nm) in MDCK MDR1.*

Al-MSNs cell internalization was evaluated by confocal microscopy to detect dye (Bodipy)-labeled Al-MSNs taken up by cells. Figure 8, A-D shows the uptake of Al-MSNs by MDCK-MDR1 cells. Only a few 170 nm Al-MSNs are visible associated with the cells, while the uptake of 70 nm Al-MSNs is very robust, which is in line with the fluorescence data. Images of MDCK-MDR1 cells incubated with Al-MSN NPs of 45 nm show the same trends, although the uptake efficiency is lower.

The uptake of Al-MSNs of 45 and 70 nm in MDCK-MDR1 cell monolayer is robust and manifested by negative permeation through the monolayer and significant permeation of the nanoparticles 170 nm was observed. Permeation of Al-MSNs has strongly reverse size-dependent value, i.e. particles with 45 nm diameter have almost remnant amount of nanoparticles in donor camera while significant amount of nanoparticles with the size 70 nm is left there. Amount of nanoparticles interacted with cells does not linearly depend on the particles size. Al-MSNs with 70 nm particles size were observed to be entrapped the most.

Previously it was established that silica nanoparticles permeate mainly through endocytosis, with low probability of transcytosis in an hCMEC/D3-based BBB model [33]. It was found that the majority of nanoparticles associated with the cells were adsorbed to the outer cell membranes, rather than being internalised by the cell monolayer. Thus, results from confocal microscopy exhibited a substantial signal which, in isolation, could be misinterpreted for nanoparticle accumulation. Cell internalization of mesoporous silica as well as alumina nanoparticles were also mentioned previously, where it was established that lower internalised doses may also activate different cellular pathways compared to those observed at higher nanoparticles doses.

Overall, confocal microscopy results support the evidence of Al-MSNs association with the MDCK-MDR1 cell layer, however we note that our results interaction of Al-MSNs with the cells could be not even through uptake, but merely adhesion on the external surface may occur. Align with the results of fluorescence measurement there remain interesting spots for future research. Also the substantial nanoparticle absorption to the outside of the cells is a concern from a purely technical standpoint, potentially making quantitative results highly dependent upon the nature of washing and other sample preparation steps.

### **3.4 Fabrication of Si-PLA nanofibers for perspective wound treatment**

Electrospun fibers with Ami immobilized in Simes and Siami were produced from PLA, with weight ratios of 1:4 and 1:2. All polymeric solutions were prepared by dissolving of PLA in a mixture of chloroform and dimethylformamide (4:1 v/v). To prepare fibers with dispersed Ami, the drug powder was dispersed in the polymeric solution and the resultant mixture left under magnetic stirring overnight before electrospinning. The fibers obtained from these formulations are



designated here as PLA-Ami. To produce composite fibers, Siam-Ami (25 or 50% of the polymer weight respectively) were dispersed in the solvent mixture and subjected to ultrasonication. The polymers were then added and left to dissolve overnight under magnetic stirring to homogenize nanoparticles in the polymer matrix solution. The produced fibers were designated as PLA-Siam25-Ami, PLA-Simes25-Ami, and PLA-Simes25-Ami according to their polymer composition. For comparison, fibers with half of the incorporated Ami in Siam and half of Ami immobilized in Simes were also prepared for the PLA blend 1:1 (w/w) (PLA-Siam50-Ami, PLA-Simes50-Ami). The compositions of all prepared mixtures are presented in Table 1. The mixtures were spun at a feed rate of 0.5 ml/h, with an applied voltage of 60 kV. The distance from the tip of the needle to the collector was set at 20 cm and a flat aluminum plate was used to collect random nanofibers. All electrospinning experiments were carried out under ambient conditions.

**Characterization of Ami-loaded and unloaded silica nanoparticles:** To achieve the goal of this study, two types of silica nanoparticles were used, namely Siam, which is commercially available, and Simes, which was synthesized by the sol-gel method and used to obtain nanofibers, which were loaded with AMI through adsorption. The obtained materials were characterized in terms of their physical properties, namely morphology (surface area, porosity, pore volume), and elemental analysis to study the AMI loading factor and electrospinning efficiency to estimate the number of loaded nanoparticles.

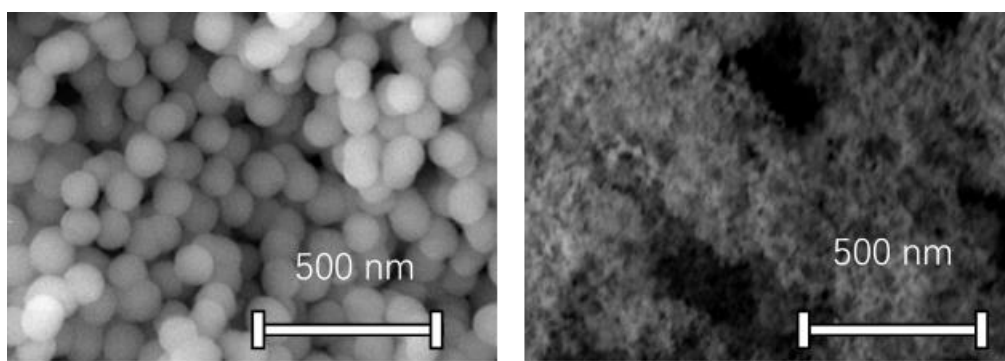


*Figure 9 SEM micrographs of Si nanoparticles (Siam, Simes).*

First, morphology of Siam and Simes was observed by SEM (see Figure 9). Fumed silica exhibited aggregated highly porous structure with the size of a single particle of 30nm, while mesoporous silica nanoparticles exhibited spherical morphology with the particle size of 200 nm.

**Morphology and fibers diameters distributions:** In the current research composite electrospun fibers composed of PLA and Simes and Siam loaded with Ami as an antibacterial compound were prepared at PLA/Si ratio 3:1 (samples PLA-25Simes-Ami and PLA-25Siam-Ami) and 1:1, w/w (samples PLA-50Simes-Ami and PLA-50Siam-Ami).

For tissue engineering scaffolds, the ideal pore size range has been found to be 150-200  $\mu\text{m}$  as reported in some previous articles [34, 35].

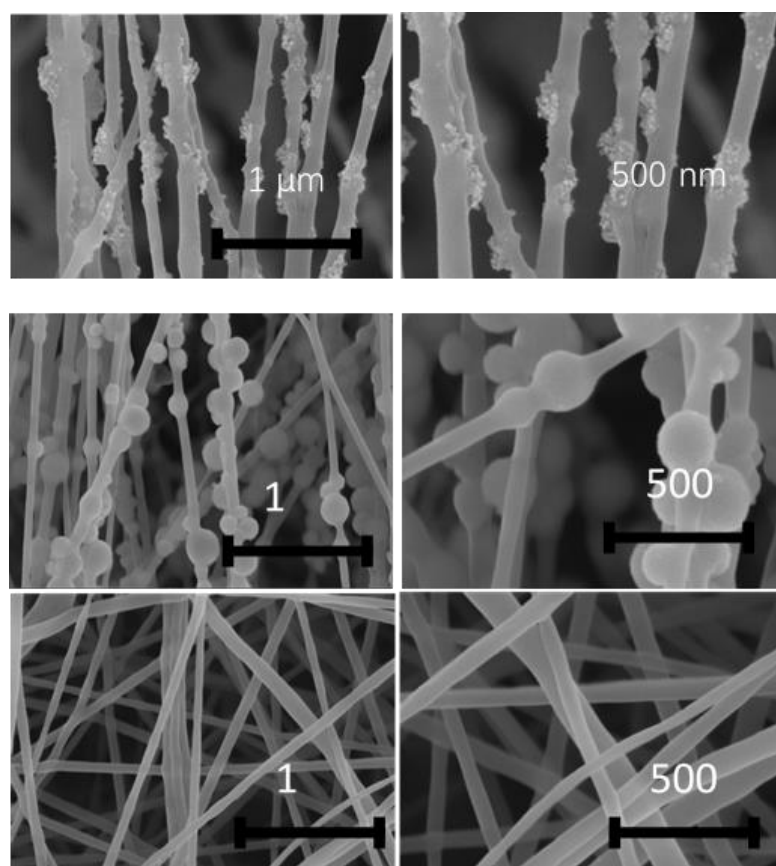


*Figure 10 SEM micrographs of the electrospun fibers, PLA-Siam-Ami, PLA-Simes-Ami and PLA respectively.*

The morphology and diameters distributions of the Ami loaded electrospun fibers are presented in Figure 10. The formulations without Si nanoparticles originated well formed fibers with smooth surfaces without beads. This formulation also generated the thinnest fibers, with an average diameter of  $97 \pm 10 \mu\text{m}$ , which is significantly lower comparing with data published earlier.

The formulations with fumed silica nanoparticles originated composite fibers with a rougher morphology, with nanoparticles aggregates distributed along the fibers, some clearly visible at their surface. The fiber diameters was higher, with PLA-Simes-Ami and PLA-Siam-Ami having 150 and 147 nm diameter and 130 and 137 nm diameter depending on the nanoparticles concentration, accordingly. According to [36] such nanofiber diameter is optimal for application of designed material in tissue engineering.

PLA-Simes-Ami nanofiners were significantly thinner ( $p < 0.05$ ), with an average diameter of  $135 \pm 7$  and  $130 \pm 3 \text{nm}$ . Fibers PLA-Simes-Ami, with part of the incorporated Ami in the free form and a part of Ami immobilized in silica nanoparticles, had a morphology different frfrom PLA-Simes-Ami (Figure 4) with an average diameter of  $150 \pm 12$  and  $147 \pm 5 \text{nm}$ , in the form of beads coated by the outer polymer layer located on the polymer streads. In the literature [36, 37], it is reported that the addition of silica nanoparticles into a polymer solution leads to an increase in both viscosity and conductivity. Since in general these two

properties have opposite effects on the diameters of electrospun fibers, the addition of silica nanoparticles can result in thicker or thinner fibers than the ones produced from the polymer solution.

**In vitro drug release studies:** This work aims to develop an Ami delivery system with prolonged and tailored release kinetics based on composite electrospun fibers comprising Ami loaded Si nanoparticles with different morphology and PLA. Si nanoparticles were selected due to the variable morphological features, i.e., pore size, surface area, pore volume, particle size, which allows to obtain electrospun fibers with very distinctive properties [38,39]. However, to the best of our knowledge, there was no specific investigation related to the impact of various morphology of Si nanoparticles on nanofibers morphology and related delimitation of bioactive compound immobilized in it. The objective of this article is to fabricate PLA nanofibers with Si nanoparticles of different morphology and investigate effect of nanoparticles on the properties of PLA nanofibers. In this work, two types of nanofibers composed by Si fumed and Si mesoporous were investigated. Besides, pure PLA composite fibers with a nano/microstructure, reported in the literature as been able to prolong the release of several drugs[39-41], were also investigated as a strategy to control Ami release kinetics. Here, Ami was immobilized in the Si nanoparticles, which in turn were embedded in the microsized PLA electrospun fibers. A referent sample was represented by Ami immobilized directly into PLA nanofibers.

The first stage of the release profiles of the composite fibers corresponds to the release of Ami in the Si-Ami particles immobilized at the surface of the fibers, in direct contact with the release medium, and/or to the release of Ami embedded directly into the structure of PLA nanofiber. The second stage corresponds to the release of Ami in the Si nanoparticles embedded inside of the nanofibers, which requires the release medium penetration through the polymer matrix and mesopores, desorption of Ami from the nanoparticles walls, and Ami diffusion out of the mesopores and through the swollen polymeric matrix.

This can be explained considering the structure of the two composite fibers. As discussed earlier, PLA-Siam-Ami nanofibers had open-pore structure, when Si nanoparticles were embedded into the fibers structure in such a way that their surface became fiber surface too, while PLA-Simes-Ami nanofibers were designed in the way that nanoparticles were completely covered by polymer. This means that GS diffusion pathway was shorter in fibers PLA-Siam-Ami nanofibers, which contributed to the increase of the release kinetics and gradual and steadily drug liberation. In this case, the balance between the length of the diffusion pathway and the diffusion rate across the polymer matrix in each fiber determined the release kinetics, resulting in PLA-Siam-Ami nanofibers fibers with a faster release kinetics., while PLA-Simes-Ami nanofibers exhibited clear two-step release kinetic with the second step occurring concomitantly with the fibers degradation. PLA-Si-nased nanofibers showed well-tailored and prolonged for more than 1 month release of a drug.

Figure 11 shows that the method of Ami immobilization (directly dispersed or loaded into nanoparticles) determined Ami release kinetics. As can be seen, the different methods of Ami incorporation resulted in fibers with totally distinct release profiles, ranging from fibers that achieved almost complete release at the end of the assay (PLA-Ami), to fibers that reached the end of the release study after a few months (PLA-Simes-Ami, PLA-Siam-Ami).

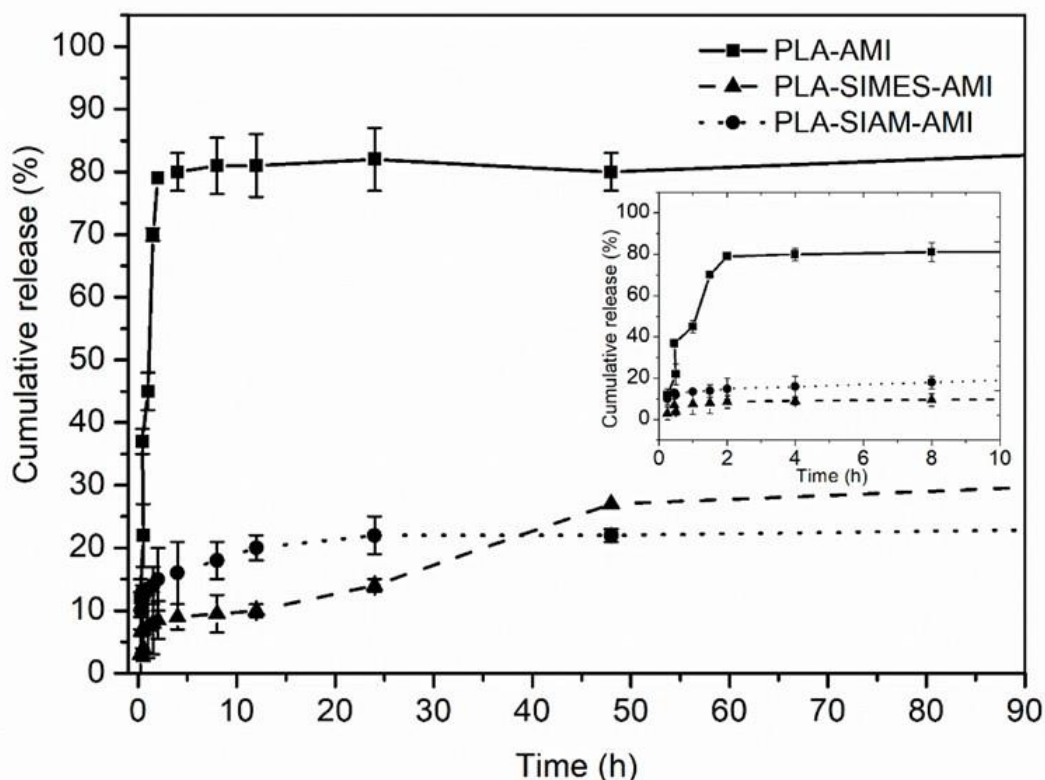


Figure 11 Ami cumulative release profiles. Comparison between composite and non-composite fibers for the three compositions.

**Antibacterial activity tests:** Resulted nanofibers were assumed to possess enhanced antibacterial properties toward Gram(+) and Gram(-) bacterial strains, so antibacterial properties of PLA-Si nanofibers were at great length studied too.

The antibacterial activity of the Ami loaded fibers against *Staphylococcus aureus* CCM 4516, *Escherichia coli* CCM 4517, *Enterococcus faecalis* CCM 3956, *Klebsiella pneumoniae* CCM 4415 and *Pseudomonas aeruginosa* CM 1961 was determined by a disk diffusion method, according to the European Committee on Antimicrobial Susceptibility Testing (EUCAST; <http://www.eucast.org>).

Samples (small amount of powder or fibers), two stacks on one Petri dish, plates in triplicate) were placed on the inoculated Mueller-Hinton agar, then the plates were incubated at 35 °C for 18 to 24 hours. After the incubation, the width of the zone inhibition for each sample was measured to the nearest millimeter on a SCAN 500 inhibition zone reader (version 8.2.0.0). As a control, fibers without Ami were also tested. Each type of fiber was tested in duplicate.

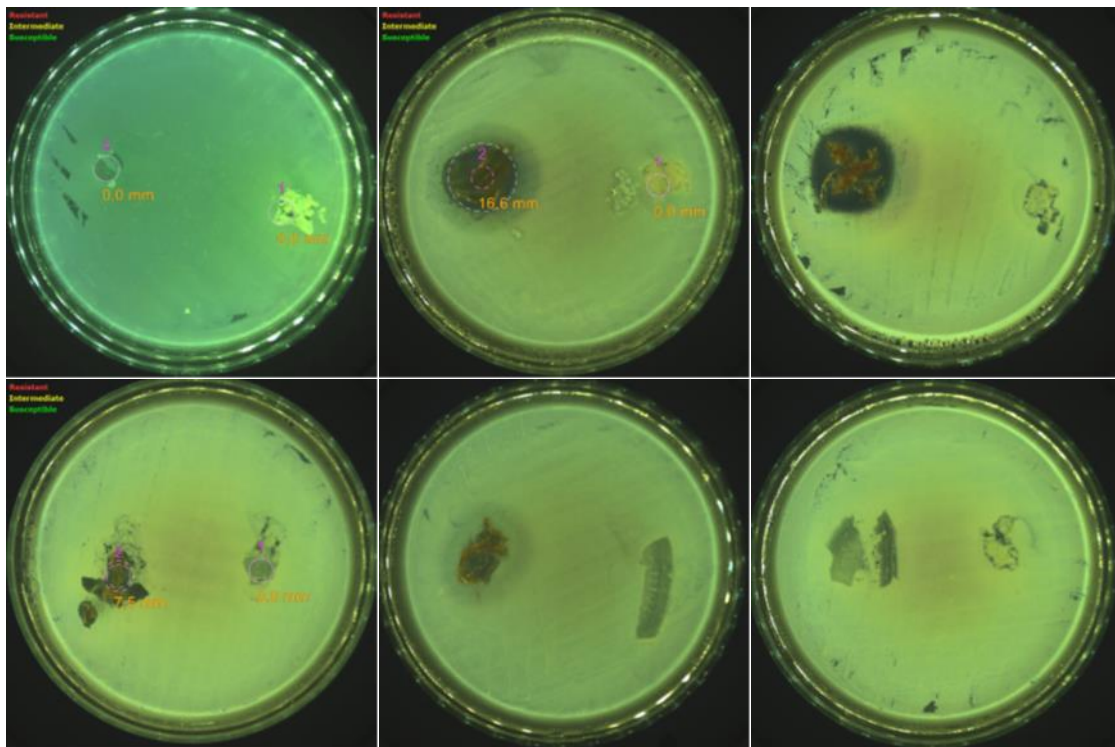


Figure 12 Examples of inhibition zones (against *St. Aureus*), images are arranged in rows from upper left corner to the right lower corner in following order: PLA, Ami, Siam-Ami, PLA-50Siam-Ami, PLA-50Simes-Ami, PLA-25Siam-Ami).

The antibacterial effect of Ami loaded fibers mats against *Staphylococcus aureus* CCM 4516, *Escherichia coli* CCM 4517, *Enterococcus faecalis* CCM 3956, *Klebsiella pneumoniae* CCM 4415 and *Pseudomonas aeruginosa* CM 1961, which are the most common agents of wound infection, was confirmed by a disk diffusion method. As can be seen in Figure 12, all Ami containing fibers produced inhibition zones, with diameters between 2.0 and 7.5 cm (the average inhibition zone diameters is the function of the average actual Ami content of the tested sample, which is in comparison with the actual content of the referent Ami sample significantly lower. In contrast, no inhibition zone was visible around the control sample (Figure 12), represented by composite fibers without Ami, proving that the observed antibacterial effect was due to Ami and not to other fibers components. As can be seen, amount of Ami present in tested materials was negligible in comparison with the referent Ami sample. It shows that presence of Silica nanoparticles by itself enhances antibacterial properties of Ami, which is in agreement with a few reported data earlier [16,17]. Antibacterial properties of nanofibers depend on the type of Si nanoparticles nanofibers are constructed with. Nanofibers built up with fumed Si nanoparticles exhibited almost two-fold higher antibacterial efficiency comparing with mesoporous one, which could be due to the faster release of antibiotic from the open-pore structure.

## 4. CONCLUSIONS

This thesis are focused on fabrication of hybrid (organic-inorganic) nanocomposites using Silica-based particles for their application in medicine. For that purpose, a detailed overview of the current state of art in the field of nanocomposite materials, with a particular attention to the preparation, characterization, biocompatibility of Silica-based nanocomposites, and conventional issues related to that matter was performed. To accomplish established aims an investigation of the impact of the experimental conditions on the Si nanoparticles properties has been performed as a background for fabrication of the controlled DDS to avoid initial burst effect through drug loading of Si particles with variable surface properties and study of the influence of its microstructure on the release of bioactive compounds through the fabrication of the DDS with increased loading capacity and enhanced water solubility and membrane permeability of the drugs with compromised bioavailability through doping of Si particles with Aluminium and study its interaction with biological barriers was accomplished.

Further, fabrication of Si-based carriers modified with CS and chitosan grafted polylactic acid as controlled drug delivery systems as the controlled DDS was performed.

Also an investigation of Si particles capability to improve antibacterial activity of the loaded drugs through preparation of the poly(lactic)acid fibers loaded with silica nanoparticles for potential application in active medical coatings and potential of Si-PLA nanofibers for sustained release of bioactive compounds was described.

A straightforward synthetic strategy to prepare pH-sensitive chitosan- and chitosan-poly(lactic) acid grafted functionalization of silica nanoparticles as suitable biocompatible nanoporous reservoirs for use in DDSs is reported. Thus, we simulated the *in vitro* loading and release of the anti-tumor drug by varying the pH value of *in vitro* system, due to the pH-dependent features of chitosan. Chitosan-functionalized nanoparticles demonstrated regular mesoporous structures, high specific surface area and guest-accommodation volume, pH response to the external environment, and good biocompatibility. PLA-grafted polymer modification of silica nanoparticles showed excellent performance in *in vitro* experiments of the loading and release of anti-cancer drug Doxorubicin hydrochloride owing to the combined advantages of chitosan, PLA and silica.

As was expected, unmodified silica carrier demonstrated rapid and full release, achieving a high level of delivery. After its functionalization release rate was characterized by the absence of an initial burst in the chitosan-modified carrier, which eventually occurred after 5 h, thereby indicating that chitosan played an important role in delaying the release of the drug; the absence of an initial burst effect also proved that Dox was located inside the system and was well protected from the external medium.

Delayed release from the silica functionalized with PLA-grafted chitosan carrier was dependent on time and pH. Grafting PLA to chitosan in trace quantities (0.458% of PLA was present in the Si-Cs-g-PLA sample, and just 4.57% in the organic coating of silica according to data from elemental analysis) significantly altered the properties of the Si-Cs-g-PLA carrier. The existence of a period of delay in release did not influence the effectiveness of such release, i.e., the ratio of Dox encapsulated and released was the same, which makes the carrier suitable for administering drugs and achieving the desired postponed effect.

The results show that the surface functionalization of Si can serve as a simple tool for controlling the loading and release of water-soluble, weak electrolyte drugs like Dox. These data mean that Si, Si-Cs, and Si-Cs-g-PLA carriers are perspective candidates for fast (Si), sustained (Si-Cs), and delayed administration of Dox.

The poor aqueous solubility and/or permeability and thereby limited bioavailability largely restricts the pharmaco-therapeutic implications of potent anticancer drugs such as methotrexate (Meth). Another chapter of this work aimed to improve and in vitro dissolution rate of Meth medicine by a invention of a carrier composed of an ordered mesoporous silica nanoparticles (MSNs) doped with Aluminium (Al-MSNs) via different experimental conditions and investigation of an impact of its microstructure on the drug bioavailability (drug liberation and model gastro-intestinal permeability). Al introduction into the structure did not lead to the drastic distortion of the shape and size of the nanoparticles.

Al-MSN nanoparticles were loaded with Meth using adsorption from solutions method. The current loading capacity for all carrier was established for concentration of carrier 1mg/ml, loading volume 3 ml and amount of carrier 20 mg. Another proportions of the adsorbent and adsorbate could drive to different values. However, the purpose of a current research was focused not on the quantitative assessment of the maximal loading capacity, but on the establishment differences that happens in drug loading while silica nanoparticles are doped with Al.

Therapeutic bioavailability of medicine is determined by two properties, dissolution profile (which we could characterise by in-vitro dissolution test ) and permeability through biological barriers, i.e. hemato-encephalic, gastro-intestinal, placental, dermal etc. barriers. Since Meth is mostly administered orally, we designed a barrier membrane permeability examination mostly relevant to gastro-intestinal permeability. MDCK-cells are well known to be a model biological model for gastro-intestinal and blood-brain permeability evaluation of medicines and were applied to investigate permeability of the immobilized Meth through the cell layer. Confocal microscopy was applied to investigate possible translocation of Al-MSNs through the cell layer.



We found that Al modification within the applied Si/Al ratio does not distort the size and shape of nanoparticles drastically. However, immobilization of Meth on the surface was successful.

Release of Meth happens in a pH- and time-dependent manner, which means that designed DDS is pH- and time-controlled.

Meth is subjected to P-glycoprotein (P-gp) mediated efflux (it is a transporter that kicks out adsorbed medicine out of the cell), resulting in lower systemic drug concentration. In particular, in our experiment the efflux ratio of free Meth was substantially high (600). However, after inclusion of Meth in Al-MSNs, inhibition of the P-gp driven efflux occurred that may contribute to increased systemic absorption, therefore enhanced permeability of Meth. Thus, SNs-based formulations effectively inhibit the P-gp efflux system of poorly water-soluble and low permeable molecules like Meth.

Additionally, we found that not only Meth is enhanced for the transportation through an experimental model of gastro-intestinal barrier, but also Al-MSNs by themselves were to the significant level translocated through the cell layer. Translocation was size-dependent, particles of the size 170 nm were better translocated compared with 35 and 70 nm particles. However, smaller particles were significantly untaken by MDCK cells.

The third chapter of the experimental part of the current thesis is to introduce novel porous electrospun fibers composed of PLA and two types of silica, i.e., mesoporous silica and fumed silica nanoparticles by electrospinning.

Electrospun polymer fibers have emerged as one of the most promising platforms for drug delivery. This status was achieved due to the relative simplicity and versatility of the electrospinning process, which permits the use and combination of a large range of polymeric materials, the production of fibers with an array of different structures and morphologies, and the development of fibrous matrices with elaborated architectures. Often, the most difficult challenge in the development of an electrospun based drug delivery system is the control of a high initial burst release, typically associated with these matrices. This characteristic, which stems from the high specific surface area of electrospun fibers, is especially problematic when the therapeutic agent is a small hydrophilic drug and/or when high drug loadings are required. An alternative approach to tackle this challenge is to prepare composite fibers comprising drug-loaded nanoparticles embedded in the electrospun polymer fibers to achieve composite materials are formed by the combination of two or more materials with different properties, that do not dissolve or blend into each other. Silica nanoparticles can improve hydrophilic properties of PLA nanofibers, which is of particular importance if highly hydrophobic therapeutic agent is implemented and/or when high drug loadings are required. It helps to manage the most difficult challenge in the development of an electrospun based drug loaded system that lies in the control of a high initial burst release, typically associated with these matrices.



Nanofibers were characterized by SEM, TGA, BET to investigate morphology, surface properties (porosity, pore size and pore volume), elemental analysis to establish ratio of Ami loading and electrospinning efficiency. Time-dependent delimitation of Ami at simulated physiological conditions and antibacterial activity toward Gram (+) and Gram (-) bacterial strains were examined to analyze perspectives of practical implementation of nanofibers in wound healing. Hydrophobic properties of nanofibers were investigated too.

PLA is a relatively hydrophobic polymer with a water contact angle in the range of 75-85° which results in a low cell affinity in biomedical applications and sometimes cause an inflammatory response from the surrounding tissue with direct contact. Incorporation of silica nanoparticles changed the hydrophobicity of nanoparticles to various extent, with amorphous silica nanoparticles resulted in the fibers of the higher diameter of 147±5 and 150±12 nm with the open-pore morphology and water contact angle 42±5 and 40±4 ° in comparison with 130±3 and 135±7 nm fibers of the close-pore morphology, and 67±7 and 59±5 ° for mesoporous silica nanoparticles, respectively.

The antibacterial effect of Ami loaded fibers mats against *Staphylococcus aureus* CCM 4516, *Escherichia coli* CCM 4517, *Enterococcus faecalis* CCM 3956, *Klebsiella pneumoniae* CCM 4415 and *Pseudomonas aeruginosa* CM 1961, which are the most common agents of wound infection, was confirmed by a disk diffusion method. Antibiotic - containing fibers produced inhibition zones, with diameters between 2.0 and 7.5. In contrast, no inhibition zone was visible around the control sample. Amount of Ami present in tested materials was negligible in comparison with the referent Ami sample. It showed that presence of Silica nanoparticles by itself enhances antibacterial properties of Ami. Antibacterial properties of nanofibers depend on the type of Si nanoparticles nanofibers are constructed with. Nanofibers built up with fumed Si nanoparticles exhibited almost two-fold higher antibacterial efficiency comparing with mesoporous one, which could be due to the faster release of antibiotic from the open-pore structure.

The results suggested that the developed composite scaffolds could be a potential candidate for tissue engineering.

These results provide a theoretical background in the control of biomedical efficiency and effectiveness of silica-polymer nanomaterials, which is an important consideration in its design and practical implementation.

## **5. SCIENTIFIC ACHIEVEMENTS AND PRACTICAL OUTCOMES**

The current doctoral thesis represent a new approach into the field of biopolymer-based silica nanocomposites for biomedical applications. The main contribution to the science of the present thesis lays in the preparation and characterization of novel biodegradable Si-Cs-g-PLA-based porous nanocomposites, nanofibers and Si nanoparticles with enhanced bioavailability of medicines.

Functionalization of Si nanoparticles by introduction of Al into the Si framework or fabrication of Si-polymer nanocomposites leads to the increase of certain valuable properties of MSNs. For instance, doping the silica framework with heteroatoms is therefore a promising strategy towards the rational design of drug release systems, which combine improved solubility and permeability level. In prospective, the heteroatom doping of mesoporous silica could be combined with varying the drug amount and carrier's textural properties in order to precisely tailor the release profiles of advanced drug delivery systems. However, it is important to note that while MSNs show great promise in drug delivery, further research is needed to optimize their design, understand long-term biocompatibility, and ensure regulatory compliance for clinical translation.

## REFERENCES

- [1] PRASAD, M. a DI NARDO, P. *Innovative strategies in tissue engineering* [online]. B.m.: River Publishers, 2015. ISBN 9788793237100. Available from: doi:10.13052/rp-9788793237100
- [2] PIGNATELLO, R. *Advances in Biomaterials Science and Biomedical Applications* [online]. B.m.: Intech Open, 2013. ISBN 978-953-51-6326-8. Available from: doi:10.5772/56420
- [3] SHIRDAR, M.R., FARAJPOUR, N., SHAHBAZIAN-YASSAR, R. a SHOKUHFAR, T. *Nanocomposite materials in orthopedic applications* [online]. 2019. ISSN 20950187. Available from: doi:10.1007/s11705-018-1764-1
- [4] SACHINJITH, K. a KRISHNA, S. A review on types of nanocomposites and their applications. *International Journal of Advance Research, Ideas and Innovations in Technology*. 2018, **4**(6), 235–236.
- [5] SINGH, N.B. a AGARWAL, S. Nanocomposites: An overview. *Emerging Materials Research* [online]. 2015, **5**(1), 5–43. ISSN 20460155. Available from: doi:10.1680/jemmr.15.00025
- [6] HASNAIN, M.S. a NAYAK, A.K. Nanocomposites for improved orthopedic and bone tissue engineering applications. In: *Applications of Nanocomposite Materials in Orthopedics* [online]. 2018, s. 145–177. ISBN 9780128137574. Available from: doi:10.1016/B978-0-12-813740-6.00008-9
- [7] BAYDA, S., HADLA, M., PALAZZOLO, S., RIELLO, P., CORONA, G., TOFFOLI, G. a RIZZOLIO, F. Inorganic Nanoparticles for Cancer Therapy: A Transition from Lab to Clinic. *Current Medicinal Chemistry* [online]. 2017, **25**(34), 4269–4303. ISSN 09298673. Available from: doi:10.2174/0929867325666171229141156
- [8] FELDMAN, D. *Polymer nanocomposites in medicine* [online]. 2016. ISSN 15205738. Available from: doi:10.1080/10601325.2016.1110459
- [9] JYOTISHKUMAR, P. *Nanocomposite materials : synthesis, properties and applications* [online]. Boca Raton, FL: CRC Press, Taylor & Francis Group, 2017. ISBN 9781482258073. Available from: doi:https://worldcat.org/title/912377600
- [10] LEE, W., KIM, D., LEE, S., PARK, J., OH, S., KIM, G., LIM, J. a KIM, J. *Stimuli-responsive switchable organic-inorganic nanocomposite materials* [online]. 2018. ISSN 1878044X. Available from: doi:10.1016/j.nantod.2018.10.006
- [11] JAWAID, M. a KHAN, M.M. *Polymer-based Nanocomposites for Energy*

- and Environmental Applications: A volume in Woodhead Publishing Series in Composites Science and Engineering* [online]. 2018. ISBN 9780081019115. Available from: doi:10.1016/C2016-0-01006-9
- [12] SAHOO, B.P. a TRIPATHY, D.K. *Properties and applications of polymer nanocomposites: Clay and carbon based polymer nanocomposites* [online]. NV-1 o. Berlin, Germany: Springer. 2017. ISBN 9783662535172. Available from: doi:10.1007/978-3-662-53517-2
- [13] RUDRAMURTHY, G.R. a SWAMY, M.K. Potential applications of engineered nanoparticles in medicine and biology: an update. *Journal of Biological Inorganic Chemistry* [online]. 2018, **23**(8), 1185–1204. ISSN 14321327. Available from: doi:10.1007/s00775-018-1600-6
- [14] GRUMEZESCU, A.M. *Biomedical Applications of Nanoparticles* [online]. Amsterdam, Netherlands: Elsevier, 2019. ISBN 9780128165065. Available from: doi:10.1016/C2017-0-04457-9
- [15] MIR, S.H., NAGAHARA, L.A., THUNDAT, T., MOKARIAN-TABARI, P., FURUKAWA, H. a KHOSLA, A. Organic-Inorganic Hybrid Functional Materials: An Integrated Platform for Applied Technologies. *Journal of The Electrochemical Society* [online]. 2018, **165**(8), B3137–B3156. ISSN 0013-4651. Available from: doi:10.1149/2.0191808jes
- [16] KHAN, I., SAEED, K. a KHAN, I. *Nanoparticles: Properties, applications and toxicities* [online]. 2019. ISSN 18785352. Available from: doi:10.1016/j.arabjc.2017.05.011
- [17] AILI, D. a STEVENS, M.M. Bioresponsive peptide–inorganic hybrid nanomaterials. *Chemical Society Reviews* [online]. 2010, **39**(9), 3358–3370. ISSN 14604744. Available from: doi:10.1039/b919461b
- [18] SHI, J., JIANG, Y., WANG, X., WU, H., YANG, D., PAN, F., SU, Y. a JIANG, Z. *Design and synthesis of organic-inorganic hybrid capsules for biotechnological applications* [online]. 2014. ISSN 14604744. Available from: doi:10.1039/c4cs00108g
- [19] GIRET, S., WONG CHI MAN, M. a CARCEL, C. Mesoporous-Silica-Functionalized Nanoparticles for Drug Delivery. *Chemistry - A European Journal* [online]. 2015, **21**(40), 13850–13865. ISSN 15213765. Available from: doi:10.1002/chem.201500578
- [20] LEE, W., KIM, D., LEE, S., PARK, J., OH, S., KIM, G., LIM, J. a KIM, J. *Stimuli-responsive switchable organic-inorganic nanocomposite materials* [online]. 2018. ISSN 1878044X. Available from: doi:10.1016/j.nantod.2018.10.006
- [21] FRANCIS, R., JOY, N., APARNA, E.P. a VIJAYAN, R. *Polymer grafted inorganic nanoparticles, preparation, properties, and applications: A*

- review [online]. 2014. ISSN 15583716. Available from: doi:10.1080/15583724.2013.870573
- [22] VIRLAN, M.J.R., MIRICESCU, D., RADULESCU, R., SABLIOV, C.M., TOTAN, A., CALENIC, B. a GREABU, M. *Organic nanomaterials and their applications in the treatment of oral diseases* [online]. 2016. ISSN 14203049. Available from: doi:10.3390/molecules21020207
- [23] KHADKA, P., RO, J., KIM, H., KIM, I., KIM, J.T., KIM, H., CHO, J.M., YUN, G. a LEE, J. Pharmaceutical particle technologies: An approach to improve drug solubility, dissolution and bioavailability. *Asian journal of pharmaceutical sciences* [online]. 2014, **9**(6), 304–316. ISSN 1818-0876. Available from: doi:10.1016/j.ajps.2014.05.005
- [24] TREWYN, B.G., SLOWING, I.I., GIRI, S., CHEN, H.T. a LIN, V.S.Y. *Synthesis and functionalization of a mesoporous silica nanoparticle based on the sol-gel process and applications in controlled release* [online]. 2007. ISSN 00014842. Available from: doi:10.1021/ar600032u
- [25] KWON, S., SINGH, R.K., PEREZ, R.A., NEEL, E.A.A., KIM, H.W. a CHRZANOWSKI, W. *Silica-based mesoporous nanoparticles for controlled drug delivery* [online]. 2013. ISSN 20417314. Available from: doi:10.1177/2041731413503357
- [26] LI, Z., ZHANG, Y.T. a FENG, N.P. Mesoporous silica nanoparticles: synthesis, classification, drug loading, pharmacokinetics, biocompatibility, and application in drug delivery. *Expert Opinion on Drug Delivery* [online]. 2019, **16**(3), 219–237. ISSN 1742-5247. Available from: doi:10.1080/17425247.2019.1575806
- [27] ŞEN KARAMAN, D., SARWAR, S., DESAI, D., BJÖRK, E.M., ODÉN, M., CHAKRABARTI, P., ROSENHOLM, J.M. a CHAKRABORTI, S. Shape engineering boosts antibacterial activity of chitosan coated mesoporous silica nanoparticle doped with silver: A mechanistic investigation. *Journal of Materials Chemistry B* [online]. 2016, **4**(19), 3292–3304. ISSN 2050750X. Available from: doi:10.1039/c5tb02526e
- [28] MAKHLOUF, A.S.H. a ABU-THABIT, N.Y. *Stimuli responsive polymeric nanocarriers for drug delivery applications, volume 1 : Types and triggers* [online]. Cambridge, MA: Woodhead Publishing, 2018. ISBN 9780081019979. Available from: doi:10.1016/C2016-0-00601-0
- [29] JIAO, Y., SHEN, S., SUN, Y., JIANG, X. a YANG, W. A functionalized hollow mesoporous silica nanoparticles-based controlled dual-drug delivery system for improved tumor cell cytotoxicity. *Particle and Particle Systems Characterization* [online]. 2015, **32**(2), 222–233. ISSN 15214117. Available from: doi:10.1002/ppsc.201400115
- [30] HAKIM, R.H., CAILLOUX, J., SANTANA, O.O., BOU, J., SÁNCHEZ-

- SOTO, M., ODENT, J., RAQUEZ, J.M., DUBOIS, P., CARRASCO, F. a MASPOCH, M.L. PLA/SiO<sub>2</sub> composites: Influence of the filler modifications on the morphology, crystallization behavior, and mechanical properties. *Journal of Applied Polymer Science* [online]. 2017, **134**(40), 45367 (12 pp.). ISSN 10974628. Available from: doi:10.1002/app.45367
- [31] VIRLAN, M.J.R., MIRICESCU, D., RADULESCU, R., SABLIOV, C.M., TOTAN, A., CALENIC, B. a GREABU, M. *Organic nanomaterials and their applications in the treatment of oral diseases* [online]. 2016. ISSN 14203049. Available from: doi:10.3390/molecules21020207
- [32] SONG, K., GUO, J.Z. a LIU, C. *Polymer-based multifunctional nanocomposites and their applications* [online]. Amsterdam: Elsevier, 2018. ISBN 9780128150672. Available from: doi:10.1016/C2017-0-01215-6
- [33] SAINT-CRICQ, P., DESHAYES, S., ZINK, J.I. a KASKO, A.M. Magnetic field activated drug delivery using thermodegradable azo-functionalised PEG-coated core-shell mesoporous silica nanoparticles. *Nanoscale* [online]. 2015, **7**(31), 13168–13172. ISSN 20403372. Available from: doi:10.1039/c5nr03777h
- [34] CHEN, P., ZHANG, C., HE, P., PAN, S., ZHONG, W., WANG, Y., XIAO, Q., WANG, X., YU, W., HE, Z., GAO, X. a SONG, J. A Biomimetic Smart Nanoplatfom as “Inflammation Scavenger” for Regenerative Therapy of Periodontal Tissue. *International Journal of Nanomedicine* [online]. 2022, **17**, 5165–5186. ISSN 11782013. Available from: doi:10.2147/IJN.S384481
- [35] HAFNER, A., LOVRIĆ, J., LAKŎ, G.P. a PEPIĆ, I. Nanotherapeutics in the EU: An overview on current state and future directions. *International Journal of Nanomedicine* [online]. 2014, **9**(1), 1005–1023. ISSN 11769114. Available from: doi:10.2147/IJN.S55359
- [36] MONCALVO, F., MARTINEZ ESPINOZA, M.I. a CELLESI, F. Nanosized Delivery Systems for Therapeutic Proteins: Clinically Validated Technologies and Advanced Development Strategies. *Frontiers in Bioengineering and Biotechnology* [online]. 2020, **8**, 89 (22 pp.). ISSN 22964185. Available from: doi:10.3389/fbioe.2020.00089
- [37] DURFEE, P.N., LIN, Y.S., DUNPHY, D.R., MUÑIZ, A.J., BUTLER, K.S., HUMPHREY, K.R., LOKKE, A.J., AGOLA, J.O., CHOU, S.S., CHEN, I.M., WHARTON, W., TOWNSON, J.L., WILLMAN, C.L. a BRINKER, C.J. Mesoporous Silica Nanoparticle-Supported Lipid Bilayers (Protocells) for Active Targeting and Delivery to Individual Leukemia Cells. *ACS Nano* [online]. 2016, **10**(9), 8325–8345. ISSN 1936086X. Available from: doi:10.1021/acsnano.6b02819

- [38] MA, Z., LI, X., JIA, X., BAI, J. a JIANG, X. Folate-Conjugated Polylactic Acid–Silica Hybrid Nanoparticles as Degradable Carriers for Targeted Drug Delivery, On-Demand Release and Simultaneous Self-Clearance. *ChemPlusChem* [online]. 2016, **81**(7), 652–659. ISSN 21926506. Available from: doi:10.1002/cplu.201600100
- [39] PARK, K. *Controlled drug delivery systems: Past forward and future back* [online]. 2014. ISSN 18734995. Available from: doi:10.1016/j.jconrel.2014.03.054
- [40] RAJALAKSHMI, R., INDIRA MUZIB, Y., ARUNA, U., VINESHA, V., RUPANGADA, V. a KRISHNA MOORTHY, S.B. Chitosan nanoparticles -an emerging trend in nanotechnology. *International Journal of Drug Delivery*. 2014, **6**(3), 204–229. ISSN 09750215.
- [41] BHARTI, C., GULATI, N., NAGAICH, U. a PAL, A. Mesoporous silica nanoparticles in target drug delivery system: A review. *International Journal of Pharmaceutical Investigation* [online]. 2015, **5**(3), 124–133. ISSN 2230-973X. Available from: doi:10.4103/2230-973x.160844.

## LIST OF FIGURES

<i>Figure 1 Schematic representation of Si particles formation.</i> .....	11
<i>Figure 2 SEM-images of silica-based nanoparticles (Silica (A), APTES-modified Si (B), Si-Cs (C) and Si-Cs-g-PLA (D)).</i> .....	12
<i>Figure 3 TEM images of silica-based particles Silica (A), Si+Dox (B), Si-Cs-g-PLA (C, D), Si- Cs (E, F, G, H).</i> .....	13
<i>Figure 4 Micrographs of the Al-doped MSNs: MSN-ATAB (a, d), MSN-Al-CTAB (b), MSN-Al-DTAB (c).</i> .....	15
<i>Figure 5 Acidity and morphology (size and shape) of the investigated samples (MSN_Al__DTAB, MSN_Al_CTAB and MSN_Al_TTAB)</i> .....	16
<i>Figure 6 Dissolution profiles of Meth from Meth-loaded Al-MSN-170nm, Al-MSN-70nm and Al-MSN-35nm and crude Meth at pH 2.0 and 8.0. Each data point represents the mean ± SD of three determinations.of Meth dissolution from Al-doped MSNs. Standard deviation was within 5% range</i> .....	18
<i>Figure 7 Transport of different Al-MSNs across MDCK MDR1 monolayers in serum-free medium. Dye-labelled Al-MSNs were applied at a concentration of 50 µg/ml. Data represent the mean apparent permeability (Papp) of MSN (n = 3) at the time point 48 hours, corrected for the loss of Al-MSNs in the upper</i>	

<i>compartment (non-permeated Al-MSNs) and associated (cellular uptake) with the cells.</i> .....	21
<i>Figure 8 Confocal images of MDCK-MDR1 cells incubated for 24 hours with Al-MSNs applied at a concentration of 50 µg/ml in serum-free medium. Nuclei stained with Hoechst 33258 (blue). Al-MSNs labeled with Bodipy (green). F-actin stained with phalloidin (red) a) reference; b) MSN-CTAB (160nm) in MDCK MDR1; c) b) MSN-DTAB (70nm) in MDCK MDR1; d) MSN-TTAB (45nm) in MDCK MDR1.</i> .....	22
<i>Figure 9 SEM micrographs of Si nanoparticles (Siam, Simes).</i> .....	24
<i>Figure 10 SEM micrographs of the electrospun fibers, PLA-Siam-Ami, PLA-Simes-Ami and PLA respectively.</i> .....	25
<i>Figure 11 Ami cumulative release profiles. Comparison between composite and non-composite fibers for the three compositions.</i> .....	27
<i>Figure 12 Examples of inhibition zones (against St. Aureus), images are arranged in rows from upper left corner to the right lower corner in following order: PLA, Ami, Siam-Ami, PLA-50Siam-Ami, PLA-50Simes-Ami, PLA-25Siam-Ami).</i> .....	28

## LIST OF TABLES

<i>Table 1 Composition of the samples with the diferent Si/Al initial ratio versus acidity and a particle size.</i> .....	16
<i>Table 2 Methotrexate storage capacities of MSNs and MSNs modified with Aluminium after interaction with Methotrexate solution</i> .....	17
<i>Table 3 Cumulative amount of Meth transported from A to B and B to A in MDCK-MDR cells. Experiment was performed in triplicates (n=3, p&lt;1)</i> .....	20



## LIST OF ABBREVIATIONS AND SYMBOLS

Al	Aluminium
BCS	Biopharmaceutical classification system
CS	Chitosan
CS-g-PLA	Chitosan grafted polylactic acid
CTAB	cetyltrimethylammonium bromide
DDS	Drug delivery system
Dox	Doxorubicin
EC	Escherichia coli
EDX	Energy-dispersive spectroscopy
FTIR	Fourier Transform Infrared
FTIR	Fourier transform infrared spectroscopy analysis
KP	Klebsiella pneumonia
LUMO	Lowest unoccupied molecular orbital
Meth	Methotrexate
MSN	Mesoporous Silica Nanoparticles
PLA	Polylactic acid
SA	Staphylococcus aureus
SE	Staphylococcus epidermidis
SEM	Scanning Electron Microscope
Si	Silica
Si-Cs-g-PLA	Silica Chitosan grafted Polylactic acid
Si-PLA	Silica grafted Polylactic acid
SN	Silica Nanoparticles
TEM	Transmission Electron Microscope
UV-Vis	Ultraviolet visible
XRD	X-Ray diffraction

# CURRICULUM VITAE

Name: **Katery(i)na O. Filatova**

Email: [filatova@utb.cz](mailto:filatova@utb.cz)

Address: T.G. Masaryka 3050, Zlin, Czech Republic, 76001

Education: **2016** - present Tomas Bata University in Zlín, Faculty of Technology. Doctoral degree studies in Chemistry and Materials technology

**2004-2009** Vinnytsia National Medical University, Ukraine, Pharmaceutical Faculty, MSc. degree Research Experience

**2016-2020** Doctoral research at Centre of Polymer Systems (CPS), Tomas Bata University, focuses on silica-polymer nanocomposites for medical applications and their biological evaluation.

**2016-2020** Internal Grant Agency of FT TBU, Research team member.

**May 2018-July 2018, June 2019- August 2019** ‘Free mover mobility’ – Enamine LTD, Institute of Physical Chemistry, NAS of Ukraine Design and Fabrication of Mesoporous Silica Nanoparticles Doped with Aluminium for improved bioavailability of Methotrexate

## **Significant experimental activities initiated and realized by a PhD candidate that were not published yet:**

1. Development and characterization of magnetic nanoparticles for waste water treatment
2. Optimization nano-and submicro-sized mesoporous silica particles with tunable size
3. ALP-functionalized mesoporous silica nanoparticles for antibody labeling in immunosensors
5. Biocompatibility of silica nanoparticles
4. Developing the procedure for the synthesis of silica-polyaniline composites
5. Stimuli-responsive PLA-grafted core-shell silica nanoclusters with potential of implementation as a carrier for biomolecules.
6. PLA microparticles for loading and liberation of antibacterial compounds.
7. Si-PLA and Chitosan-PLA porous scaffolds loaded with amikacin.

## LIST OF PUBLICATIONS

1. Mikusova, Nikola, Humpolicek, Petr, Ruzicka, Jan, Capakova, Zdenka, Janu, Kristyna, Kasparikova, Vera, Bober, Patrycja, Stejskal, Jaroslav, Koutny, Marek, Filatova, Katerina, Lehocky, Marian, Ponizil, Petr. Formation of bacterial and fungal biofilm on conducting polyaniline. *Chemical Papers*. 2017. vol. 71, no. 2, pp. 505-512. ISSN 2585-7290. DOI: 10.1007/s11696-016-0073-8.
2. Golovan, Alina P., Krupska, Tatiana V., Filatova, Katerina O., Sedlarik, Vladimir, Humpolicek, Peter, Borisenko, Mykola V., Pakhlov, Eugeny M., Turov, Vladimir V. The Silica-Amizon composite system and its properties. *Butlerov Communications*. 2016. vol. 16, no.7. DOI: jbc-02/16-47-7-62.
3. Kurmach, Mykhailo M, Konyshva, Kateryna M., Filatova, Kateryna, Sotnik, Svitlana O., Gavrilenko, Konstantin S., Andreev, O.V., Shvets, Oleksij Vasylyovich. Properties of hierarchy zeolite obtained from obsidian and perlite. *Theoretical and Experimental Chemistry*. 2022. vol. 57, no. 6. DOI: 10.1007/s11237-022-09715-8.
4. Strasakova, Monika, Pummerova, Martina, Filatova, Kateryna, Sedlarik, Vladimir. Immobilization of caraway essential oil in a polypropylene matrix for antimicrobial modification of a polymeric surface. *Polymers*. 2021. vol. 13, no. 6. ISSN 2073-4360. DOI: 10.3390/polym13060906.
5. Durpekova, Silvie, Filatova, Kateryna, Cisar, Jaroslav, Sedlarik, Vladimir. A novel hydrogel based on renewable materials for agricultural application. *International Journal of Polymer Science*. 2020, vol. 2020. DOI: 10.1155/2020/8363418.
6. Glinka, Marta, Filatova, Kateryna, Kucinska-Lipka, Justyna, Domincova-Bergerova, Eva, Wasik, Andrzej, Sedlarik, Vladimir. Encapsulation of amikacin into Microparticles based on low-molecular-weight polylactic acid and polylactic acid-co-polyethylene glycol. *Molecular Pharmaceutics*, 2021, vol. 18, no. 8, pp. 2986-2996. ISSN 1543-8384/2021. DOI: 10.1021/acs.molpharmaceut.1c00193.
7. Glinka, Marta, Filatova, Kateryna, Kucinska-Lipka, Justyna, Sopik, Tomas, Domincova-Bergerova, Eva, Mikulcova, Veronika, Wasik, Andrzej, Sedlarik, Vladimir. Antibacterial porous systems based on polylactide loaded

with amikacin. *Molecules*. 2022. vol.27, no. 20. ISSN 1420-3049 DOI: 10.3390/molecules27207045.

8. Filatova, Kateryna, Domincova Bergerova, Eva, Kazantseva, Natalia, Masar, Milan, Suly, Pavol, Sopik, Tomas, Cisar, Jiri, Durpekova, Silvie, Sedlarik, Vladimir. Design and Fabrication of Electrospun PLA-Based Silica-Modified Composite Nanofibers with Antibacterial Properties for Perspective Wound Treatment. Online. *Polymers*. 2023. vol. 15, no. 12. ISSN 2073-4360. DOI: 10.3390/polym15173500.

### **Conference proceedings:**

1. Filatova, K., Di Martino, A. Sedlarik, V. Surface modification of silica with biodegradable amphiphilic polymer for controlled release applications. In *the International Conference on Materials and Technology (24. ICM&T)*.
2. Filatova, K., Sedlarik, V. Effect of silica modification with chitosan and chitosan-g-poly(lactic acid) on release trend of doxorubicin. In *The 8<sup>th</sup> international conference on nanomaterials - research and application*.
3. Filatova, K., Sedlarik, V. Polymer-coated Silica particles for controlled drug delivery. In *Newgen Zlín Workshop and WG Meeting On Hydrogel/ Biomineralized Biomaterial for Bone Tissue Regeneration*. ISBN: 978-80-7454-623-5.
4. Filatova, K., Sedlarik, V. Nano- and submicro-sized mesoporous silica particles with tunable size and porosity as perspective biopharmaceutically active excipients. In *Pharmaceutical Regulatory Affairs*. ISSN: 2167-7689.
5. Filatova, K., Sedlarik, V. An optimization of the large-scale room-temperature syntheses of mesoporous silica particles with tunable size and porosity for advanced pharmaceutical implementation. In *NANOCON 2017 Conference Proceedings-International Conference on Nanomaterials*.

# **Nanocomposites for medical applications**

## **Nanokompozity pro medicínské aplikace**

Doctoral Thesis Summary

Published by: Tomas Bata University in Zlín,  
nám. T. G. Masaryka 5555, 760 01 Zlín.

Edition: published electronically

Typesetting by: Kateryna O. Filatova, Ph.D.

This publication has not undergone any proofreading or editorial review.

Publication year: 2024

First edition

ISBN: 978-80-7678-275-4

